Grand Valley State University
ScholarWorks@GVSU

Masters Theses Graduate Research and Creative Practice

12-2017

Effect of Arm Motion on Standing Lateral Jump Performance

Arif Ahmed Sohel
Grand Valley State University

Follow this and additional works at: https://scholarworks.gvsu.edu/theses

Part of the Engineering Commons

ScholarWorks Citation

Sohel, Arif Ahmed, "Effect of Arm Motion on Standing Lateral Jump Performance" (2017). *Masters Theses*. 869.
https://scholarworks.gvsu.edu/theses/869

This Thesis is brought to you for free and open access by the Graduate Research and Creative Practice at ScholarWorks@GVSU. It has been accepted for inclusion in Masters Theses by an authorized administrator of ScholarWorks@GVSU. For more information, please contact scholarworks@gvsu.edu.

Effect of Arm Motion on Standing Lateral Jump Performance

Arif Ahmed Sohel

A Thesis Submitted to the Graduate Faculty of

GRAND VALLEY STATE UNIVERSITY

In

Partial Fulfillment of the Requirements

For the Degree of

Master of Science in Engineering

School of Engineering

December 2017

Dedication

To my parents, MD. Salim Mia and Mrs. Khorsheda Akter, and my wife Afsana Alam, for their selfless and relentless support to my pursuit of higher studies.

Acknowledgments

I would like to thank my committee members for all their support and assistance in completing this project. Special thanks to my advisor, Dr. Blake Ashby for guiding me throughout the investigation process and the writing of my thesis. Also, special thanks to Dr. Gordon Alderink for educating me about the motion capture lab and helping me in data collection. I would also like to thank the Statistical Consulting Center at Grand Valley State University for helping me in developing a statistical model of this project.

Abstract

Previous jumping studies have examined the role of arm swing in vertical and horizontal long jump performance, but none have been found which studied the role of arm swing in standing lateral jumps. The purpose of this study was to investigate the effect of arm motion on standing lateral jump performance and to examine the biomechanical mechanisms that may explain differences in jump distance.

A series of lateral jump experiments was performed for two jump cases (free and restricted arms) in which six participants jumped laterally for maximum distance from two in-ground force platforms. A motion capture system collected 3D position data for lateral jumps with free and restricted arms. Inverse dynamics analyses were performed on three-dimensional (3D) models for free and restricted arm jumps and the joint angular velocities, moments, powers, and work values were compared. The mechanisms enabling any performance improvement of lateral jump performance due to free arm motion were also investigated.

Results showed that free arm motion improved standing lateral jump performance by 29%. This improvement was due to the increase in take-off velocity and increase in the lateral and vertical displacement of the center of gravity at take-off and touchdown. The improved take-off velocity and position of the center of gravity at take-off was due to a 33% increase in the work done by the body in jumps with free arm movement. This increase in work in free arm jumps compared to restricted arm jumps was found in both upper and lower body joints with the largest improvements (> 30 J) occurring at the lower back, right hip, and right shoulder.

The increase in work performed at the lower back and right hip could not be explained by joint torque augmentation resulting from the slowing of joint angular velocities due to arm

movement. Other mechanisms involved in enabling this work improvement can be discovered from further investigations of this movement. For example, computer simulation studies could provide additional insight into the motor control strategies employed in lateral jumps with free and restricted arm movement.

Table of Contents

List of Figures

List of Tables

1 Introduction

Jumping in multiple directions is a common human movement required in many sports like basketball, volleyball, football, baseball, and soccer. Jump performance depends on strength, power, and coordination of the entire body. Many researchers have analyzed jumping to reveal important factors related to jumping performance. Jumping requires more extensive coordination of upper body and lower body movements than many other fundamental human movements. The objectives of this study were to study the effect of arm swing on standing lateral jumps and reveal motor coordination principles that enable any performance enhancement due to the free arm movement.

The role of arm movement in vertical and forward jump performance has been investigated in many previous studies. Several studies showed that the free arm movement has a positive effect on standing vertical jump performance (Luhtanen and Komi, 1978; Shetty and Etnyre, 1989; Harman et al., 1990; Feltner et al., 1999; Lees and Barton, 1996). Investigators also studied standing jumps for distance to demonstrate the benefit of the arm movement on jump distance and explore the mechanism underlying the improved performance (Ashby and Heegaard, 2002; Wu et al., 2003; Ashby and Delp, 2006; Hara et al., 2008). In addition, researchers have analyzed the motor coordination of lower extremity movement in lateral jumping in a few studies (Lee et al., 2012; Sinsurin et al., 2013; Aizawa et al., 2016). However, all the lateral jumping studies involved either one-leg jumping or one-leg landing. No studies have examined standing two-leg lateral jumps with two leg landing or the role of arm movement on lateral jump performance.

Arm swing has been shown to improve vertical jump performance in many experimental and simulation studies. Arm swing has been shown to improve vertical jump height by raising the center of gravity height and increasing take-off velocity by 9% to 12.7% (Luhtanen et al., 1978;

Harman et al., 1990; Shetty and Etnyre, 1989; Feltner et al., 1999). Arm swing in vertical jumping has also been reported to improve jump performance by increasing the total body momentum (Lees et al., 1996) and vertical ground reaction forces (Harman et al., 1990; Shetty et al., 1989). Researchers have also suggested that arm swing improves jump performance by causing additional downward forces on the upper body thereby enhancing muscle force production by slowing the shortening velocity of the lower body extensor muscles (Harman et al., 1990; Feltner et al., 1999). Two more recent studies (Lees et al., 2004; Cheng et al., 2008) showed improved performance in free arm vertical jumps. The mechanisms behind this performance improvement were analyzed more extensively by examining some common theories ("joint torque augmentation" theory and "pull" theory, which will be discussed in detail in Chapter 2). The "joint torque augmentation" theory has been called into question by Lees et al. (2004), but they supported the "pull" theory for jump performance improvement due to arm swing. However, Cheng et al. (2008) supported both theories because they found that both mechanism (joint torque augmentation and pull) were responsible for improved jump performance in free arm jumps. Domire et al. (2010) did a simulation energy analysis and suggested that both joint torque augmentation mechanism and energy contribution (for pull mechanism) from the arm swing were factors that contributed to increased jump performance.

Ashby and Heegaard (2002) showed that free arm movement improved standing long jump performance by 21.1% compared to restricted arm jumps. This result was explained by the increased take-off velocity of the center of gravity (CG) and the change in CG position relative to the foot at take-off and touchdown. Wu et al. (2003) showed that jump performance improved 20% to 50% for jumps with arm motion compared to jumps without. Hara et al. (2008) examined the effects of directional arm swing on standing long jump performance and found that jump performance, work done by the joints, and velocity of CG at take-off were greater when the direction of arm swing was in the jumping direction. In another study, the mechanism of the improved jump performance for free arm motion in standing long jump was examined with optimal control simulations (Ashby and Delp, 2006). The results supported the “hold back,” “impart energy,” and “joint torque augmentation” theories, which will be discussed in detail in Chapter 2.

All previous lateral jumping studies have been conducted with either one-leg jumping or one-leg landing. Lee et al. (2012) conducted a study on double leg jump with single leg landing to investigate the effect of jump landing directions on sagittal plane kinematics, kinetics, energy dissipation. They found knee and ankle joints as the dominant contributors to energy dissipation for forward, diagonal, and lateral jumping. In an experimental study of one-leg jump landings, Sinsurin et al. (2013) found that peak knee valgus angle was greater when jumping in lateral and diagonal directions than in the forward direction.

Many previous studies have provided insight into the motor coordination strategies for standing vertical or forward jumps and the effect of arm swing on performance. Although numerous sports require explosive jumping movements in the lateral direction, no study has documented the biomechanics related to jumping in the lateral direction of two legs. The purpose of this study was to investigate the standing two-leg lateral jump and examine the role of arm movement on lateral jump performance. Specifically, the following questions were addressed:

1. To what extent does arm movement improve performance in standing lateral jumps?

2. What biomechanical mechanisms may explain any performance improvement due to arm motion in standing lateral jumps?

The results of this study increase the general understanding about the factors that affect jumping performance in multidirectional jumping and provide insight into the biomechanical mechanisms that enable any performance improvement in lateral jumps with arm movement. Ultimately, these insights could prove helpful in the training of individuals who desire to improve their physical performance or in the prevention or rehabilitation of injuries.

2 Background

Several previous studies analyzed the biomechanics of human jumping involving arm movement and showed the effect of arm swing on vertical jump performance (Lees et al., 2004; Cheng et al., 2008; Nagano et al. 2008; Feltner et al., 1999). The effect of arm motion on jump performance was also investigated for the standing long jump (Ashby and Heegaard, 2002; Wu et al., 2003; Ashby and Delp, 2006) and the mechanism of the enhanced performance due to arm swing has been explained by three main theories: “joint torque augmentation” theory, “impart energy” theory, and “hold back” theory (Lees et al., 2004; Ashby et al., 2006; Cheng et al., 2008). Other researchers have investigated one-leg lateral and directional horizontal jump performance (Lee et al., 2012; Aizawa et al., 2016). The effect of arm swing on standing lateral jumps has not been investigated in any previous study.

2.1 Arm Swing Effect on Jump performance

Jumping performance is a key concern in any type of jumping and depends on many factors including muscle strength, functional symmetry, initial body position, and techniques for performance optimization (Mackala et al., 2013). Coordination of take-off angle and take-off velocity has also been identified as an important factor for maximum vertical jumping performance

(Wakai and Linthorne, 2005). Luhtanen and Komi (1978) first identified arm swing as a key factor for vertical jumping performance, and several other studies have verified this (Shetty and Etnyre, 1989; Harman et al., 1990; Feltner et al., 1999; Lees and Barton, 1996). The role of arm swing has also been investigated for standing forward jumps with a significant positive effect on performance demonstrated (Ashby and Heegaard, 2002; Wu et al., 2003; Ashby and Delp, 2006; Hara et al., 2008).

The reasons why arm movement increases jump performance have been investigated in many previous studies. Arm swing has been shown to increase take-off velocity. Several theories have been proposed to describe the mechanisms that enable this. The theory of “force transmission,” first introduced by Payne et al. (1968) contends that the ground reaction force is increased during the arm acceleration phase due to a greater downward force on the body. This increased ground reaction force creates greater impulse, which increases the vertical velocity of the CG of the body at take-off. This theory was described as a simple idea to explain the reason behind the increased take-off velocity due to arm swing (Dapena, 1993; Payne et al., 1968). Later an experimental study found no relation between the net joint force at the shoulder and the vertical ground reaction force (Lees et al., 2004). This finding was corroborated by a simulation study (Cheng et al, 2008) therefore, the force transmission theory has been marked as questionable.

The increased take-off velocity in jumps with free arm jump movement has also been explained by another theory called the “joint torque augmentation” theory (Feltner et al., 1999). This theory suggests that the additional downward force on the trunk due to upward acceleration of the arm slows lower body joint extension velocities, which decreases shortening velocities of the hip and knee extensor muscle groups, enabling them to produce greater force consistent with the force-velocity properties of muscle (Feltner et al., 1999; Harman et al., 1990). This theory was further supported by the studies of Hara et al. (2006). Lees et al. (2004) found that joint torque augmentation was associated with energy that is stored and later released to enhance jump performance. In a simulation standing long jump study, Ashby and Delp (2006) found increased joint torque, power, and work due to arm movement slowing joint extension velocities at the hip and ankle, but not at the knee. Cheng et al. (2008) and Domire et al. (2010) in their vertical jump simulation studies found torque augmentation at the hips only, thus providing additional support for the "joint torque augmentation" theory.

Improved jump performance due to arm motion has also been explained by the "pull" theory (Harman et al., 1990). According to this theory, during the start of deceleration of the arms near take-off, the increased relative velocity of arms enables them to pull the trunk, which causes energy transfer from the arms to the rest of the body. This theory is supported by the experimental study of Lees et al. (2004) and simulation study of Cheng et al. (2008). Ashby and Delp (2006) provided support for this theory in a simulation study of standing long jump and rephrased it as the "impart energy" theory. They found by doing a work analysis that additional energy imparted to the system by muscles crossing the shoulder joints was the most significant factor in increasing the velocity of the CG at take-off. Domire et al. (2010) also did a simulation study for vertical jumping and found that the pull mechanism contributed to performance improvement.

Based on a standing long jump study, Ashby and Heegaard (2002) introduced the "hold back" theory as an explanation for decreased performance in jumps with restricted arm movements (Ashby and Heegard, 2002). This theory suggests that during restricted arm jumps, without the ability to rotate the arms backwards during the flight phase to help position the body for landing, the jumpers had to "hold back" during the take-off phase in order to avoid excessive forward rotation. The evidence for this theory was the earlier decline of the vertical ground reaction force in restricted arms jumps and the development of a counterproductive backwards moment of the ground reaction force about the CG.

2.1.1 Vertical Jump Studies

The role of arm motion in vertical jumping has been studied extensively. Luhtanen and Komi (1978) conducted a study to determine the segmental contributions to vertical jump performance. This study showed that the arm swing made a 10% contribution in the take-off velocity of vertical jump. The most important conclusion of the study was that a multibody movement like jumping needs proper muscle coordination and proper training to increase jumping performance.

Shetty and Etnyre (1989) conducted a kinetic and kinematic study to determine the contribution of arm movement to the vertical jump. Maximum vertical ground reaction force, total work done, total power exerted by the jumper, body velocity at take-off, and impact force at touchdown were calculated for free and restricted arm movement. The average maximum force, work done, power, and take-off velocity were greater in free arm jumps than restricted arm jumps. Shetty and Etnyre concluded that trained jumpers who use their arms more effectively have better vertical jumping performance. Another important finding was that the impact energy at landing was smaller in free arm jumps than restricted arm jumps. The reason behind the lower impact forces in free arm jumps was unclear, which called for further investigation.

Harman et al. (1990) conducted a study to determine the effects of arm swing and countermovement on vertical jump performance. After doing four different types of jumps in a combination of arm-swing/no-arm-swing and countermovement/no-countermovement, they found that arm swing contributed up to 10% of the take-off velocity of both countermovement and non-countermovement vertical jumps, which was similar to the findings of Luhtanen and Komi (1978). This study also found that both arm swing and countermovement significantly improved the jump height, but arm swing had a greater effect. Arm swing increased the height of the CG at take-off (when feet leave the ground) and after the take-off (the peak CG height). But, countermovement had only peak CG height increase after the take-off. Arm swing increased the peak CG height (after take-off) by 21%, increasing the vertical ground reaction impulse 10%. However, countermovement had only 6% increase in the peak CG height (after take-off) due to the 3% increase of vertical ground reaction impulse. The combination of both arms swing and countermovement enhanced vertical jump performance by increasing the net vertical ground reaction impulse.

Lees and Barton (1996) used the relative momentum principle to assess the free limbs' contribution to countermovement jump performance. In the countermovement jump, the free arms were found to generate a relative momentum of 30.9 Ns, which was 12.7% of the peak total vertical momentum of the body.

Feltner et al (1999) conducted a study on countermovement vertical jumps with and without arm motion of 25 volleyball players to determine the role of arm movement. They found that the vertical velocity and height of the body CG at take-off was greater with arm motion, which led to greater jump height. The authors concluded that the body CG height increase contributed 43% and velocity increase contributed 57% to the total performance improvement of free arm vertical jumps. The total peak jump height was 9% greater in jumps with free arm motion.

Lees et al. (2004) found that jump performance increased due to increased CG height (28%) and take-off velocity (72%). They examined the various proposed theories for performance improvement due to free arm motion in the vertical jump and suggested that none of the previously introduced theories ("joint torque augmentation" theory, "impart energy" theory and "pull" theory) exclusively explained the improved jump performance due to arm swing. The improved jump performance for free arm motion was due to the series of mechanisms, which were operating together. The authors claimed that the increased take-off velocity occurred from the energy buildup by the free arm motion at an early stage and transferred to the rest of the body during the later stage of the jump. This additional energy was generated from extra work done by muscles at the shoulder joints, elbow joints, and hip joints. This increased jump performance by increasing kinetic and potential energies of the body at take-off. The storing and releasing of energy from the muscles around the joints also resulted in pulling on the body by an upward force acting on the trunk at the shoulder.

Cheng et al. (2008) did a simulation study to examine the prevailing theories explaining vertical jump performance improvement. According to the findings of this investigation the "force transmission" theory was questionable because no vertical ground reaction force change was found due to the force on shoulder joint from arm movement. The "joint torque/work augmentation" theory was demonstrated at the hip joints, but not at the knee and ankle joints. The "pull/impart energy" theory was demonstrated because about the half of the additional energy produced in jumps with arm motion was generated at the shoulder joints. This simulation study did not count elbow joint for energy calculation and modeled the forearm and upper arm as a single segment.

More recently, several researchers conducted experimental and simulation studies to understand the mechanism of enhanced jump performance for free arm motion in vertical jumps (Lees et al., 2007; Domire et al., 2010; Blache et al., 2013). Energy analyses were done to check the validity of the previously introduced "pull" or "impart energy/energy transfer" theories. Lees et al. (2007) showed that the developed kinetic energy of free arm motion resulted in a potential energy increase at take-off, to store and return energy from the lower limb muscles and to pull on the rest of the body. From simulation results, Domire et al. (2010) and Blache et al., (2013) found that both mechanisms contributed to the performance improvement due to arm swing. Arm swing allowed the hip extensors to generate more force by slowing down the hip extension velocities and also perform greater work. In addition, the shoulder muscles generated a significant amount of work, which contributed to one-third of the enhanced performance of free arm vertical jumps.

2.1.2 Standing Long Jump Studies

It has also been shown that the use of arm motion during standing long jump increases jump performance. A study by Ashby and Heegard (2002) found that free arm motion increased jump performance by 21.2% over jumps with restricted arm motion. The greater performance in free arms jumps was due to greater take-off velocities of the CG, increased horizontal and vertical displacement of the CG at take-off, and increased horizontal distance between the toes and CG at touchdown.

Motion analysis was done to determine the effects of arm motion, initial knee angle, and anthropometrics on jump performance (Wu et al., 2003). A series of eight jumps for each of 34 female participants was collected for jumps with a combination of free and restricted arm motion and with initial knee angles of 45° and 90°. It was found that the jump performance with free arm motion was 20% to 50% greater than with restricted arm motion depending on initial knee flexion. Additionally, the jump distance with the 90° initial knee angle was 20% longer than with the 45° initial knee angle. The results also showed that the angle of the CG velocity at take-off was not an important factor in jump performance and anthropometrics (height, shank length, thigh circumference, shank circumference, leg length, and body weight) played a less important role in jump performance. Jumpers with longer legs did not always show better performance. Jumpers with shorter legs, or shorter people who have proper coordination and technique of using countermovement and arm motion, were able to jump farther than the taller people who did not use their arm motion in effective ways.

The mechanisms that enable arm motion to improve performance in the standing long jump were analyzed in a simulation study (Ashby and Delp, 2006). In this study, optimal control simulations were developed to determine the joint torque activations for maximizing jump performance of free and restricted arm motion jumps. The results supported the three main theories ("hold back," "impart energy," and "joint torque augmentation"). In restricted arm jumps, evidence of ''holding back'' was demonstrated during the propulsive phase by reduced activation levels in order to allow the segments to be properly positioned for landing. In free arm jumps, the ability to swing the arms during the flight phase allowed for greater levels of activation of the lower body joint actuators. The greater activations allowed for greater joint torques, joint powers, and joint work. The additional work done by the shoulder actuator in the free arm jumps increased the total energy of the system resulting in greater velocity and greater CG position at take-off, thus validating the "impart energy" theory. Joint torque augmentation occurred at the hip and ankle joints due to the reduction of angular velocity caused by arm swing. However, the joint torque was lower at the knee during the propulsive phase. Since the increased joint torques at the hip and ankle were achieved because of lower angular velocities, the resulting joint power and work (joint power integrated over time) may or may not have been greater. In this simulation study, the work done was greater at the ankle and hip and lower at the knee in jumps with free arm movement.

Hara et al. (2008) performed a study on standing long jumps in forward and backward directions to investigate the differences in jump performance for directional arm swing. The study was performed by doing a kinematic and kinetic analysis of jumping data of seven participants. Each subject was instructed to jump for six different cases (forward jump-no arm swing, forward jump-forward arm swing, forward jump-backward arm swing, backward jump-no arm swing, backward jump-forward arm swing, and backward jump-backward arm swing). Results indicated that the jumping performance, work done by the joints and velocity of CG at take-off were increased when the arm swing had the same direction as jumping direction. The study also showed that the integrated electromyography (iEMG) of the biceps femoris during the hip power development phase was significantly larger in the cases of similar direction jumping and arm swing. The lower activations as demonstrated by the iEMG results may be the evidence of the participants "holding back" during the jumps with no arm swing and in the jumps with opposite direction arm swing.

A review of the literature revealed that all previous standing long jump or forward jump investigations (Ashby and Heegard, 2002; Wu et al., 2003; Ashby and Delp, 2006; Hara et al., 2008; Filush and Ashby, 2012; Vlietstra, 2014) were done based on a 2D assumption. Only one study had experimentally investigated forward jumping using a 3D model (Hickox, 2014; Hickox et al., 2016). In this study, 3D and 2D models were compared to check the validity of the 2D, sagittal plane assumptions for the standing long jump. The results showed good agreement between the 2D and 3D models for the lower body, but significant differences were found in the upper body because of the significant motion of the arms outside of the sagittal plane during the jumps. Their 3D model also captured the difference between left and right sides of the body that were not observable with the 2D model. Hickox et al. (2016) concluded that the planar motion assumption may be sufficient for standing long jump studies where only the lower body motion is important, but in the case where upper body motion is vital, the 3D model is more appropriate.

2.2 Lateral Jump Studies

A thorough literature review discovered many studies that investigated lateral jumping (Meylan et al., 2010a; Meylan et al., 2010b; Lee et al. 2012; Hewit et al., 2012a; Hewit et al., 2012b; Sinsurin et al. 2013; Lockie et al., 2013; Mornieux et al., 2014; Lockie et al., 2015 Aizawa et al. 2016). Meylan et al. (2010a) conducted kinematic analyses to compare the difference of vertical ground reaction forces between three types of unilateral jumps: vertical, forward, and lateral. Their comparison study of eccentric (i.e., negative vertical velocity phase of body CG) and concentric (i.e., positive vertical velocity phase of body CG) vertical ground reaction force and concentric peak power among three jumps revealed that the eccentric peak force was 14-16% greater and concentric peak power was 45-51% greater in vertical countermovement jumps than in forward and lateral countermovement jumps. No significant differences were observed between forward and lateral countermovement jumps for these three variables. The authors also tried to establish the best kinetic predictors of jump performance in the vertical, forward, and lateral directions of motion. Through statistical correlations, they found that concentric peak vertical power, forward concentric peak power, and eccentric peak vertical ground reaction forces were the best predictors of jump performance for all three jump types. The authors also did eccentric kinematics variable comparisons and found that in vertical countermovement jumps, eccentric peak velocity of CG (body) was 0.15 m/s ($p < 0.05$) and 0.06 m/s ($p < 0.05$) greater compared to horizontal countermovement jumps and lateral countermovement jumps, respectively (Meylan et al., 2010b).

Lee et al. (2012) conducted a study to investigate the effect of different jump-landing directions on sagittal plane kinematics, kinetics, and energy dissipation. Participants were instructed to do double leg jumps to a height equivalent to 50% of their maximum vertical jump height and maintain their balance after landing on one foot for forward, diagonal, and lateral jumps. Three major findings emerged: 1) the knee and the ankle joints were the major energy dissipaters for a single-leg jump-landing (all three directions), 2) the knee joints were the dominant energy dissipaters for forward and diagonal jump-landing directions, and 3) the ankle joint was the dominant energy dissipater for the lateral jump-landing direction. Participants were found to change body position (joint angles and angular velocities) and energy dissipation at knee and ankle joints to maintain the same level of ground reaction force (GRF) for all three jump directions. The authors concluded that landing strategy changed across three landing directions to maintain the same level of shock attenuation (GRF).

Hewit et al. (2012a) quantified and compared average symmetry indexes across jumping directions (vertical, lateral, and forward) and variables (jump distance and height, peak force, and peak power). Sub-elite netball players performed single leg (for both legs) countermovement jumps from force plates in vertical, horizontal, and lateral directions with two-leg landings. They found the variation in the magnitude of the average symmetry indexes ranged from 3.1% (peak force) to 11.4% (peak power), which depends on the variable and direction used to quantify the asymmetry.

Hewit et al. (2012b) investigated the leg asymmetry in athletes. This study assessed limb asymmetry (power, force, and distance/height jumped), the reliability of single-limb multidirectional assessments, and expected magnitudes of asymmetry in non-injured and injured athletes, which can be used for future injury prevention programming. They concluded that a threshold of 15% leg asymmetry is appropriate to identify the athletes who are prone to lower limb injury. Additional training to correct the leg asymmetry can be provided to the athletes who have leg asymmetry greater than the threshold of 15%.

Sinsurin et al. (2013) conducted a study to examine the peak knee valgus angle during one leg jump landing in various directions. Eighteen male participants jumped from a 30 cm-high platform in four directions (forward, 30° diagonal, 60° diagonal, and lateral). The study found that the peak knee valgus angles were greater when landing in lateral and diagonal directions than when landing in the forward direction.

Mornieux et al. (2014) analyzed the adaptation in motor control in response to task unpredictability during lateral jump movements. Participants jumped to the right with three different landing modalities: 1) without any perturbation (stable condition), 2) with an initial perturbation to the right (sliding condition), and 3) with an initial perturbation to the left (counteracting condition) for two settings: 1) participants knew the landing modalities prior to the jumps (predictable) and 2) participants did not know the landing modalities prior to the jumps (unpredictable). They found greater hip joint abduction in the unpredictable jump setting compared to the predictable jump setting. For the sliding landing modality, hip flexion and knee flexion decreased at touchdown in the unpredictable setting compared to the predictable setting. During the stable landing modality, the knee joint abduction increased after initial ground contact in the unpredictable setting compared to the predictable setting. Their results support the hypothesis that pre-programmed motor activity depends on the predictability of the landing modality during lateral jumps.

Lockie et al. (2013) investigated the interaction between dynamic stability and single leg lateral jump distance measured by Star Excursion Balance Test (SEBT) for each leg. They found dynamic stability significant for the dominant leg in lateral jumps. In another study, Lockie et al. (2015) studied the relationship between dynamic stability and multidirectional jumping. Their results showed a limited relationship between unilateral dynamic stability and multidirectional jump performance. Seven out of 36 correlations were found significant for the comparison between excursion distances and jump performance and no significant differences were observed in jump performance between better and lesser dynamic stability group. Their results also highlighted the complex interaction between physiological, biomedical, and technical factors related to lower body multidirectional movements.

Aizawa et al. (2016) did a study to clarify the correlation between kinematics and impact forces during lateral jump landings. Results showed that the peak vertical ground reaction force during single leg lateral jump landings was related to knee flexion during the flight phase and pelvic anterior inclination during the landing phase. Their findings suggest that the decreased knee flexion 100 ms before landing and increased pelvic anterior inclination during the landing phase increased the vertical impact force.

Previous studies have shown that arm swing improves jump performance in vertical and forward jumps. Data suggest that increased take-off velocity and improved positioning of CG at take-off with free arm movement are the primary reasons for improved jump performance. Free arm movement appears to allow lower limb muscles to increase internal work, while the shoulder and elbow muscles provide additional work in vertical and forward jumps. The mechanisms for this work improvement due to arm swing have been described using a few theories (“joint torque augmentation”, “impart energy”, “force transmission” and “hold back”). However, arm swing effect on lateral jump performance has not been investigated. Several lateral jump studies have been conducted to answer research questions related to jumping symmetry, motor control technique, and dynamic stability. However, all previous lateral jumping studies involved either one leg jumping or one leg landing. No studies have examined standing two-leg jumps with two-leg landings. This is the first study to investigate standing lateral jumps of two legs with two-leg landings. The main purpose of this study is to study the arm swing effects on jumping performance of two-leg lateral jumps and to investigate the mechanism underlying any performance change.

3 Method

3.1 Experimental Design

This was a quasi-experimental design that compared distance jumped and selected kinematic and kinetic variables of the arms, trunk, and lower extremities, for jumps with or without the use of arms. A series of two-leg lateral jump trials was conducted in the Biomechanics and Motor Performance Laboratory at Grand Valley State University using an eight-camera Vicon motion capture system and two in-ground force plates. The cameras recorded the 3D positions of reflective markers placed on the skin and clothing of each participant throughout each jumping trial. Force plates were used to determine the ground reaction forces and locations of the center of pressure during the take-off phase of the jumps. All jumping trials also were documented with video. Participants were instructed to jump for the maximum distance for each trial for two different types of jumps: free arm lateral jumps and restricted arm lateral jumps. The participants were instructed to take-off and land with both feet at approximately the same time.

3.1.1 Participant Selection

Six physically active adult males (age: 26.7 ± 2.4 years; weight: 85.5 ± 10.6 kg, and height: 1.823 ± 0.097 m, mean ± standard deviation), volunteered to participate in this study. The participants were included if they were physically active at least once a week with no persisting back, neck, ankle, knee, hip, shoulder, or elbow injuries. Participants were excluded if a physician had placed limitations on their activity levels for physical or medical reasons. All potential participants completed a written survey (attached as Appendix D) with questions about their age, height, and weight; frequency, duration, and level exertion of physical activity; past injuries along with the persisting effects of those injuries; and whether any limitations had been placed on their current physical activity by a physician. The protocol for this study was reviewed and approved by the Human Research Review Committee at Grand Valley State University.

3.1.2 Equipment

Jumping trials were captured with a 3D motion capture system (Vicon Motion System Ltd, LA, CA) using eight cameras (8 MX-T40), a set of reflective markers, and two in-ground AMTI force plates (Advanced Mechanical Technology Inc., Watertown, MA). The three-dimensional positions of the reflective markers were recorded using infrared LED strobe lights of the cameras at 120 Hz, and force data was recorded at 1200 Hz. Vicon Nexus v2.5 software was used to process the marker positions and force plate data. The processed data were exported using Vicon Nexus into CSV file format for further analysis in MATLAB R2017a (MathWorks, Natick, MA), Wolfram Mathematica 11.1.1 (Wolfram Research, Inc., Champaign, IL), and SAS® OnDemand for Academics (SAS Institute Inc., Cary, NC, USA).

3.1.3 Model Selection

In this study, significant motion occurred in all three planes and the motion of the upper extremities was of particular importance, so using a 3D model was the appropriate choice. A pre-developed 3D model from the Hickox (2014) study based on these following assumptions was used:

1. Segment lengths are constant.
2. The CG of each segment is located on the segment long axis.
3. CG and moment of inertia are constant with respect to the anatomical reference frame of the segments.
4. There is no relative translation at the joints between adjacent segments.

There were 12 segments in this model: feet, shanks, thighs, pelvis, trunk, upper arms, and forearms (Figure 1). The anatomic reference frames were chosen based on Ren et al. (2008) and recommendations by the International Society of Biomechanics (ISB) (Wu et al., 2002; Wu et al., 2005) (Appendix A). In the neutral anatomic position, all x-axes were in an anterior direction, all y-axes were along the segments longitudinal direction, and all z-axes were pointing towards the right side.

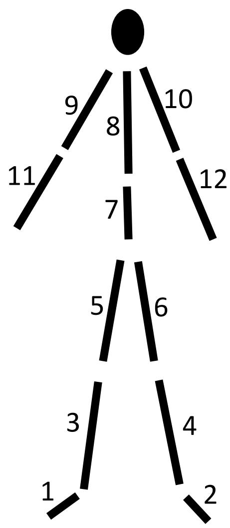

- 1 & 2: feet
- 3 & 4: shanks
- 5 & 6: thighs
- 7: pelvis
- 8: head, neck, and trunk
- 9 & 10: upper arms
- 11 & 12: forearms

Figure 1: Twelve segments of 3D jumping model

3.1.4 Marker Selection

Similar to Hickox (2014), the biomechanical model used in this study included 53 markers (Figure 2). The markers were placed on the skin, shoes, and clothing of each participant with double-sided tape. The marker placements were verified by an experienced physical therapist. A cluster of three markers was used on the thigh and upper arm segments required for the

Symmetrical CoR Estimation (SCoRE) method to determine hip and shoulder joint center locations (Ehrig et al., 2006). In the selected marker set, an additional marker was placed on the shoulder blade to make the model asymmetric, which assisted in labeling and gap processing. The Hickox marker set included greater trochanter markers; however, they were not used in this study. To reduce the soft tissue artifact, bony landmarks were used as much as possible for marker placement. The complete set of marker names and locations is listed in Appendix B.

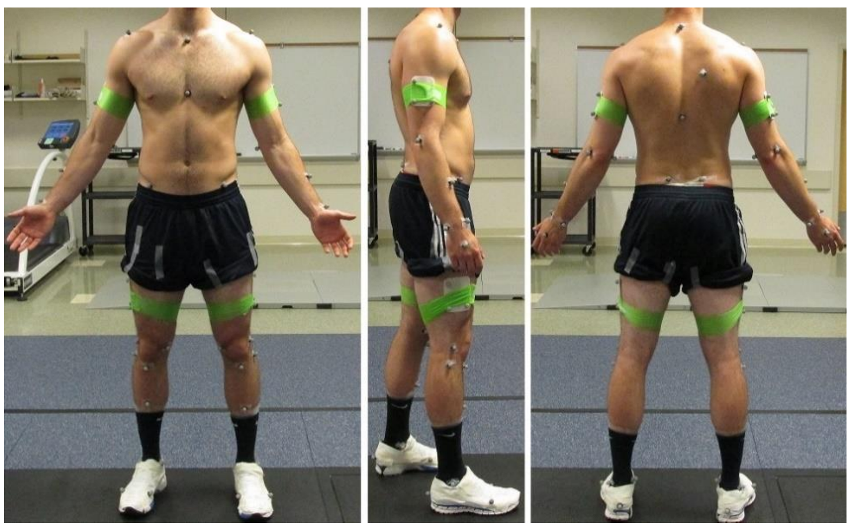

Figure 2: Full body marker set of 3D jump model

3.1.5 Data Collection

The participants were directed to warm up by jogging at a self-selected comfortable speed for 5 minutes on a treadmill. They were then allowed to stretch, if desired. Participants were also instructed to practice each type of jump three to four times prior to data acquisition. For each participant, separate static trials data were collected while standing on the force plates to determine each participant's weight and to capture the complete marker set for joint center calculations and segment parameters. For the SCoRE method, four trials were collected in one cycle of a flexion/extension, abduction/adduction, circumduction movement for each hip and shoulder joint. Two types of lateral jumps to the right: 1) with free arms and 2) with restricted arms (with arms akimbo – hands on the hips and elbows turned outward) were performed. For data acquisition, each participant was asked to stand with one foot on each force plate and jump as far as possible once given a verbal signal. He performed each type of lateral jump six times alternating each type of jump. Participants were allowed to rest between jumps, if desired, to minimize any fatiguing effects.

3.2 Data Analysis

Captured 3D position data for static and dynamic trials were labeled and gaps in trajectory data were filled using spline, pattern, or rigid body software algorithms in Vicon Nexus v2.5 software. Processed data was exported from Nexus as a CSV file, which was read by MATLAB. The force plate data was subsampled at a 1:10 ratio to match markers data collection frequency 120 Hz. Take-off time was defined by the time when ground reaction force went to zero for both force plates. The start of the jump was considered as 1.2 s before take-off, which is the time for all jumps before any movement began when the total lateral ground reaction force was still close to zero and the total vertical ground reaction force was still close to bodyweight. The remaining data before and after the take-off was clipped and an extra frame of data on either end of jump cycle was left to calculate velocities and accelerations in the kinematic analysis. In MATLAB, the clipped marker position data and force plate data were filtered using a 4^{th}-order, dual pass, zero-lag Butterworth filter with a cutoff frequency of 10 Hz. The segmental parameters (length, CG locations, mass and moments of inertia) were calculated from the static trials based on the segment definitions and parameters from Zatsiorsky et al. (1990) and de Leva (1996), and a similar procedure was followed as described by Hickox (2014)

3.2.1 Joint Center Estimation

Joint center locations were calculated using the functional SCoRE method (Ehrig et al., 2006) as described by Hickox (2014). The ankle, knee, elbow, and wrist joint centers were calculated as the midpoint between the medial and lateral joint markers by taking an average over the entire static trial (Hickox, 2014). The L3/L4 position was determined based on average anthropometric data from Zatsiorsky et al. (1990) (adjusted by de Leva, 1996), and a similar procedure was followed to calculate L3/L4 and lower back joints as described by Hickox (2014).

3.2.2 Kinematic Analysis

In MATLAB, technical reference frames for each segment were created from filtered static trial data (global position data). Calculated global static joint centers were transformed to technical reference frames to determine the local positions of the joint centers for each segment. These local joint centers were averaged for all the static data frames resulting in a single position of the joint centers relative to each segment's local technical reference frame. For the dynamic trials, technical reference frames for each segment with the same markers used for the static trials were created again for each time frame. Rotation matrices generated from these dynamic technical reference frames were used along with the on local joint center positions calculated from the static trials to determine the dynamic joint centers in the global reference frame at each point in time. These dynamic global joint centers along with other dynamic marker data were used to create anatomical reference frames for each segment as described in Appendix A. Then the anatomic reference frames were used to determine segment rotation matrices. The Euler angle equations for each segment were determined based on XYZ rotation order shown in Appendix C. These Euler angle equations and segment rotation matrices were used to calculate three angles (α, β, and γ) for each segment.

By differentiating the calculated three Euler angles of each segment, three non-orthogonal angular velocity components $\dot{\alpha}$, $\dot{\beta}$, and $\dot{\gamma}$ were determined.

$$\dot{\alpha} = \frac{\alpha_{i+1} - \alpha_{i-1}}{2\Delta t} \tag{1}$$

$$\dot{\beta} = \frac{\beta_{i+1} - \beta_{i-1}}{2\Delta t} \tag{2}$$

$$\dot{\gamma} = \frac{\gamma_{i+1} - \gamma_{i-1}}{2\Delta t} \tag{3}$$

These non-orthogonal angular velocity components were transformed to orthogonal angular velocity components in the segment anatomical reference frame by using Equation 4. Here R_y and R_z are individual rotation matrices for each rotation about the y and z axes, respectively (Appendix C)

$$\begin{bmatrix}\omega_x\\ \omega_y\\ \omega_z\end{bmatrix} = R_z \cdot R_y \cdot \begin{bmatrix}\dot{\alpha}\\ 0\\ 0\end{bmatrix} + R_z \cdot \begin{bmatrix}0\\ \dot{\beta}\\ 0\end{bmatrix} + \begin{bmatrix}0\\ 0\\ \dot{\gamma}\end{bmatrix} \tag{4}$$

Performing the matrix multiplications in Equation 4 results in the following three equations for the angular velocity components for each segment (expressed in the anatomic reference frames):

$$\omega_x = \dot{\beta}\cos\alpha\cos\gamma + \dot{\gamma}\sin\alpha \tag{5}$$

$$\omega_y = -\dot{\beta}\cos\gamma\sin\alpha + \dot{\gamma}\cos\alpha \tag{6}$$

$$\omega_z = \dot{\beta}\sin\gamma + \dot{\alpha} \tag{7}$$

By differentiating the calculated three Euler angles of each segment twice, three non-orthogonal angular acceleration components $\ddot{\alpha}$, $\ddot{\beta}$, and $\ddot{\gamma}$ were determined.

$$\ddot{\alpha} = \frac{\alpha_{i+1} - 2\,\alpha_i + \alpha_{i-1}}{\Delta t^2} \tag{8}$$

$$\ddot{\beta} = \frac{\beta_{i+1} - 2\,\beta_i + \beta_{i-1}}{\Delta t^2} \tag{9}$$

$$\ddot{\gamma} = \frac{\gamma_{i+1} - 2\,\gamma_i + \gamma_{i-1}}{\Delta t^2} \tag{10}$$

The angular acceleration components for each segment (expressed in the anatomic reference frame) were calculated by time differentiating the angular velocity equations (equations 5, 6 and 7):

$$\alpha_x = \ddot{\beta}\cos\alpha\cos\gamma + \ddot{\gamma}\sin\alpha - \dot{\alpha}\,\dot{\beta}\sin\alpha\cos\gamma - \dot{\gamma}\cos\alpha\,(\dot{\beta}\sin\gamma - \dot{\alpha}) \tag{11}$$

$$\alpha_y = -\ddot{\beta}\sin\alpha\cos\gamma + \ddot{\gamma}\cos\alpha - \dot{\alpha}\,\dot{\beta}\cos\alpha\cos\gamma - \dot{\gamma}\sin\alpha\,(\dot{\beta}\sin\gamma - \dot{\alpha}) \tag{12}$$

$$\alpha_z = \ddot{\beta}\;\dot{\gamma}\cos\gamma + \ddot{\beta}\sin\gamma \tag{13}$$

The segment rotation matrices of anatomic reference frames were used to determine the joint rotation matrices by using the following equation.

$$R_{d/p} = (R_{d/G})\,(R_{p/G})^T \tag{14}$$

Where,

$R_{d/p}$ is joint rotation matrix from the proximal segment to distal segment

$R_{d/G}$ is a segment rotation matrix from global to distal segment reference frame, and

$R_{p/G}$ is a segment rotation matrix from global to proximal segment reference frame

The Euler angle equations for each joint were determined based on XYZ rotation order shown in Appendix C. These Euler angle equations and joint rotation matrices were used to calculate three angles for each joint. The sign convention for the joint angles was similar to Hickox (2014) (Appendix B). From the calculated Euler angles (α, β, and γ), joint angular velocities were determined by following the similar procedure (using equation 1 to 7) of calculating segmental angular velocities.

CG position for each segment was determined in anatomical reference frame from static trial data as described by Hickox (2014). In dynamic trials, local (in anatomical reference frame) CG positions were transformed to the global reference frame to determine the dynamic CG positions. These dynamic CG position data were numerically differentiated using the center difference formula to calculate the linear acceleration of CG for each segment.

$$a_x = \frac{x_{i+1} - 2x_i + x_{i-1}}{\Delta t^2} \qquad (15)$$

$$a_y = \frac{y_{i+1} - 2y_i + y_{i-1}}{\Delta t^2} \qquad (16)$$

$$a_z = \frac{z_{i+1} - 2z_i + z_{i-1}}{\Delta t^2} \qquad (17)$$

3.2.3 Inverse Dynamics

An inverse dynamics method was used to calculate the joint forces and internal moments for each body segment. The generic forms of the equations for the 3D model, which were used for every segment are given below. Here, Figure 3 represents every segment except the pelvis and trunk. The pelvis and trunk both have two distal joints (e.g., left and right hips and shoulders) where the regular segments have only one.

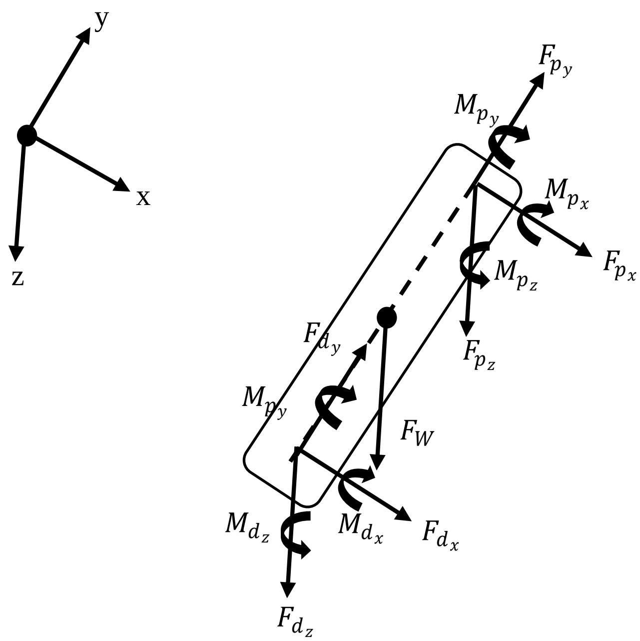

Figure 3: Segmental force and moment diagram for 3D model (Winter, 2009)

The general inverse dynamics equations for forces of 3D model in terms of global reference frame are in the following form,

$$\sum F_x = F_{p_x} + F_{d_x} = ma_x \tag{18}$$

$$\sum F_y = F_{p_y} + F_{d_y} = ma_y \tag{19}$$

$$\sum F_z = F_{p_z} + F_{d_z} - F_w = ma_z \tag{20}$$

Where,

F_{p_x}, F_{p_y}, F_{p_z} are proximal joint force components,

F_{d_x}, F_{d_y}, F_{d_z} are distal joint force components,

F_W is the gravitational force on the segment,

m is segment mass, and

a_x, a_y, a_z are acceleration components of segment's CG.

The general form of inverse dynamics moment equations for the 3D model in terms of the anatomic reference frame are given below:

$$\sum \vec{M}_G = \vec{M}_d + \left(\vec{l}_d \times \vec{F}_d\right) + \vec{M}_p + \left(\vec{l}_p \times \vec{F}_p\right) = \begin{Bmatrix} I_x\alpha_x + (I_z - I_y)\omega_y\omega_z \\ I_y\alpha_y + (I_x - I_z)\omega_z\omega_x \\ I_z\alpha_z + (I_y - I_x)\omega_x\omega_y \end{Bmatrix} \tag{21a}$$

For the pelvis and trunk, equation 21b should be used instead of equation 21a because these two segments had two distal points for each.

$$\sum \vec{M}_G = \vec{M}_{d_L} + \left(\vec{l}_{d_L} \times \vec{F}_{d_L}\right) + \vec{M}_{d_R} + \left(\vec{l}_{d_R} \times \vec{F}_{d_R}\right) + \vec{M}_p + \left(\vec{l}_p \times \vec{F}_p\right) = \begin{Bmatrix} I_x\alpha_x + (I_z - I_y)\omega_y\omega_z \\ I_y\alpha_y + (I_x - I_z)\omega_z\omega_x \\ I_z\alpha_z + (I_y - I_x)\omega_x\omega_y \end{Bmatrix} \tag{21b}$$

Where,

$\vec{M}_d$ is the distal joint moment,

$\vec{M}_{d_L}$ is the left distal joint moment,

$\overrightarrow{M}_{d_R}$ is the right distal joint moment,

$\overrightarrow{M}_p$ is the proximal joint moment,

$\vec{l}_d$ is the position vector between CG and distal joint,

$\vec{l}_{d_L}$ is the position vector between CG and left distal joint,

$\vec{l}_{d_R}$ is the position vector between CG and right distal joint,

$\vec{l}_p$ is the position vector between CG and proximal joint,

I_x, I_y, I_z segmental principal moments of inertia about x, y, z axes,

ω_x, ω_y, ω_z segmental angular velocity components about x, y, z axes, and

$\alpha_x, \alpha_y, \alpha_z$ segmental angular acceleration components about x, y, z axes.

Using equation (18) to (21) for each segment six equations can be generated. For a 12-segment 3D model, there are 72 equations with 78 unknowns.

72 equations:

–ΣF_x, ΣF_y, ΣF_z, ΣM_{G_x}, ΣM_{G_y}, ΣM_{G_z} for segment 1

–ΣF_x, ΣF_y, ΣF_z, ΣM_{G_x}, ΣM_{G_y}, ΣM_{G_z} for segment 2

–……………………………........................

–…………………………………………….

–ΣF_x, ΣF_y, ΣF_z, ΣM_{G_x}, ΣM_{G_y}, ΣM_{G_z} for segment 12

78 unknowns:

–F_{gx}, F_{gy}, F_{gz}, x_{COPx}, x_{COPy}, x_{COPz} for both left and right feet

–R_{1x}, R_{1y}, R_{12z}, M_{1x}, M_{1y}, M_{1z}

– R_{2x}, R_{2y}, R_{12z}, M_{2x}, M_{2y}, M_{2z}

–...

–...

– R_{11x}, R_{11y}, R_{11z}, M_{11x}, M_{11y}, M_{11z}

Force plates data provides the values for 12 unknowns (F_{gx}, F_{gy}, F_{gz}, x_{COPx}, x_{COPy}, x_{COPz}) for both left and right feet, which reduces the number of unknowns from 78 to 66 and makes the system over-constrained. “Bottom-up” and “top-down” inverse dynamics calculations were used as described by Hickox (2014), Vlietstra (2014), Filush and Ashby (2012), and Ashby et al. (2015). The upper part of the model was solved from each hand to the shoulder and the lower part of the model was solved from the ground to the lower back. The indeterminacy was resolved by not using the six equations of trunk segment.

3.2.4 Joint Power and Work

To understand the contributions of muscles at various joints to performance improvement, a work analysis was required. The net joint power generated or absorbed at each segment of the 3D model was calculated with the following equation:

$$P_{joint} = P_d + P_p \tag{22}$$

Where,

P_p is generated or absorbed power at the joint on the proximal segment, and

P_d is generated or absorbed power at the joint on the distal segment.

P_d and P_p were calculated by using the following equations in the segment anatomical reference frames (Winter, 2009):

$$P_d = \vec{M}_d \cdot \vec{\omega}_d = M_{d_x}\omega_{d_x} + M_{d_y}\omega_{d_y} + M_{d_z}\omega_{d_z} \qquad (23)$$

$$P_p = \vec{M}_p \cdot \vec{\omega}_p = M_{p_x}\omega_{p_x} + M_{p_y}\omega_{p_y} + M_{p_z}\omega_{p_z} \qquad (24)$$

After getting the net joint power, joint work was calculated by numerically integrating the joint power over the 1.2 s before take-off at the ankle, knee, hip, lower back, shoulder, and elbow joints. The total body work was obtained by summing all of the joint work terms.

3.2.5 Effect of center of gravity (CG) position differences on jump distance

Any increase in the vertical CG position at take-off or any decrease in the vertical CG position at landing results in additional lateral jump distance. The amount of this increase in lateral distance as a result of differences in the vertical CG positions at take-off and touchdown was calculated using the following projectile formulas.

Lateral change in CG position, $\Delta y = V_{yo} t$ (25)

Lateral CG velocity at takeoff, $V_{yo} = V_o \cos\theta$ (26)

Vertical CG velocity at takeoff, $V_{zo} = V_o \sin\theta$ (27)

Vertical change in CG position, $\Delta z = V_{zo} t - \frac{1}{2}\, g t^2$ (28)

Where,

Lab y-axis (positive) is the lateral jumping direction

Lab z-axis (positive) is the vertical direction (i.e., perpendicular to lab floor)

θ is take-off angle (angle of the CG velocity vector relative to the y-axis in the y-z plane),

t is time,

V_o is take-off velocity magnitude, and

g is gravitational acceleration.

The additional jump travel time for any improvement in the vertical CG positions at take-off and touchdown was calculated using equation 27 and 28.

Additional jump travel time, $t = \frac{V_o \; \sin\theta - \sqrt{{V_o}^2 \; \sin\theta^2 - 2\, g\, \Delta z}}{g}$ (29)

For this additional jump travel time, the additional lateral jump distance covered by the participants was calculated using equation 25, 26 and 29.

Additional lateral jump distance,

$$\Delta y = V_o \ \cos\theta \ \frac{V_o \ \sin\theta - \sqrt{V_o{}^2 \ \sin\theta^2 - 2\, g\, \Delta z}}{g} \qquad (30)$$

Using equation 30, for any vertical CG improvement Δz at take-off and landing, the resulting lateral jump distance improvement Δy was calculated.

3.2.6 Statistical modeling

The statistical SAS Studio server, SAS Institute Inc. 2015. SAS® OnDemand for Academics (SAS Institute Inc., Cary, NC, USA) was used to create repeated measures mixed models for comparisons between free and restricted arm jumps for each parameter. Each model had three classes: subject (1, 2, 3, 4, 5, 6), jump type (free and restricted arms) and trial (1, 2, 3, 4, 5, 6). The subject effect was not counted and the results for each parameter were calculated for free and restricted arm jumps. Four jump trials (two of each jump type for one subject) out of 72 were not captured properly. These gaps in the data set were properly handled by the statistical models within the SAS software. All calculated results are reported as the least square mean ± the 95% confidence interval (CI). The p values are reported for each comparison between free and restricted arm jumps, with a value of 0.05 used to indicate statistical significance for each comparison.

4 Results

4.1 Jump distance

Arm swing allowed participants to jump 29% ($p < 0.0001$) farther over restricted arm jumps. The mean jump distances for restricted and free arm jumps were 1.231 ± 0.141 m and 1.587 ± 0.141 m, respectively. Jump distance was defined by the lateral distance between the right head of the 5th metatarsal (RMT5) at take-off and the left head of the 5th metatarsal (LMT5) at touchdown.

4.2 Center of Gravity (CG) kinematics

The 29% jump performance improvement in free arm jumps was due to the increase in the take-off velocity, increases in the lateral and vertical position of the CG relative to the right foot at take-off, and differences in the lateral and vertical position of the CG relative to the left foot at touchdown. The mean take-off velocity of the CG for free arm jumps was 3.20 ± 0.17 m/s, which was a 13% increase ($p < 0.0001$) over the restricted arm jumps average take-off velocity of 2.83 ± 0.17 m/s. There was no significant difference ($p = 0.6240$) between take-off angle for free (39.6 ± 1.7 º) and restricted (39.2 ± 1.7 º) arm jumps. At take-off, the mean lateral position of the CG relative to RMT5 was 0.324 ± 0.038 m for free arm jumps, which was 7.2 cm greater ($p < 0.0001$) than for restricted arm jumps (0.252 ± 0.038 m). The mean CG height at take-off for free arm jumps (1.117 ± 0.012 m) was 2.4 cm greater ($p < 0.0001$) than for restricted arm jumps (1.093 ± 0.012 m). Also, the touchdown lateral position of LMT5 relative to the CG was 4.1 cm greater ($p < 0.0001$) for free arm jumps (0.147 ± 0.015 m) than for restricted arm jumps (0.106 ± 0.015 m).

Table 1: Comparison of key kinematic and kinetic parameters (mean ± 95% CI)

	Free arms	**Restricted arms**	**p-value**
Jump distance (m)	1.587 ± 0.141	1.231 ± 0.141	<0.0001
lateral position of CG w/r RMT5 at TO (m)	0.324 ± 0.038	0.252 ± 0.038	<0.0001
CG height at TO (m)	1.117 ± 0.012	1.093 ± 0.012	<0.0001
CG velocity at TO (m/s)	3.20 ± 0.17	2.83 ± 0.17	<0.0001
angle of TO velocity (º)	39.6 ± 1.7	39.2 ± 1.7	0.6240
lateral position of LMT5 w/r CG at TD (m)	0.147 ± 0.015	0.106 ± 0.015	<0.0001
CG height at TD (m)	0.988 ± 0.015	0.999 ± 0.014	0.0335
peak VGRF left foot (BW)	1.35 ± 0.04	1.37 ± 0.04	0.2191
peak VGRF right foot (BW)	1.11 ± 0.03	1.04 ± 0.03	<0.0001
time of peak VGRF left foot (s)	-0.23 ± 0.02	-0.25 ± 0.02	0.0445
time of peak VGRF right foot (s)	-0.15 ± 0.02	-0.17 ± 0.02	0.0126
peak LGRF left foot (BW)	0.58 ± 0.04	0.52 ± 0.04	<0.0001
peak LGRF right foot (BW)	0.37 ± 0.02	0.31 ± 0.02	<0.0001
time of peak LGRF left foot (s)	-0.15 ± 0.01	-0.15 ± 0.01	0.8674
time of peak LGRF right foot (s)	-0.07 ± 0.01	-0.07 ± 0.01	0.1278
peak VGRF total (BW)	2.38 ± 0.05	2.32 ± 0.05	0.019
time of peak VGRF total (s)	-0.18 ± 0.02	-0.21 ± 0.02	0.0004
peak LGRF total (BW)	0.84 ± 0.05	0.75 ± 0.05	<0.0001
time of peak LGRF total (s)	-0.13 ± 0.01	-0.13 ± 0.01	0.5029
NOTE: RMT5 = right 5th metatarsal head; LMT5 = left 5th metatarsal head; TO = take-off; TD = touchdown; BW = body weight VGRF = vertical ground reaction force; LGRF = lateral ground reaction force;			

4.3 Ground reaction forces (GRF)

The vertical (lab z-axis) and lateral (lab y-axis) ground reaction forces (GRF) on the left foot and right foot were normalized to the body weight (BW) of each participant to make meaningful comparisons between free and restricted arm jumps. Total (left foot + right foot) vertical ground reaction forces (VGRF) and lateral ground reaction forces (LGRF) were also calculated (Figure 4).

The peak left-foot LGRF was 11% ($p < 0.0001$) greater in free arm jumps (0.58 ± 0.04 BW) than in restricted arm jumps (0.52 ± 0.04 BW), but the time of peak LGRF was basically the same ($p = 0.8674$) for free arm (-0.15 ± 0.01 s) and restricted arm (-0.15 ± 0.01 s) jumps (Figure 4). For the right foot, the peak LGRF in free arm jumps (0.37 ± 0.02 BW) was 18% greater ($p < 0.0001$) than in restricted arm jumps (0.31 ± 0.02 BW). The time of peak LGRF did not differ significantly ($p = 0.1278$) between free (-0.07 ± 0.01 s) and restricted (-0.07 ± 0.01 s) arm jumps.

The magnitude of peak left foot VGRF did not differ significantly ($p = 0.2191$) between free (1.35 ± 0.04 BW) and restricted (1.37 ± 0.04 BW) arm jumps, but the time of peak VGRF was about 0.02 s later ($p = 0.0445$) for free (-0.23 ± 0.02 s) than for restricted (-0.25 ± 0.02 s) arm jumps (Figure 4). The magnitude of the peak right-foot VGRF was 6% greater ($p < 0.0001$) in free arm jumps (1.11 ± 0.03 BW) than in restricted arm jumps (1.04 ± 0.03 BW). The peak VGRF time for the right foot occurred 0.02 s later ($p = 0.0126$) in free arm jumps (-0.15 ± 0.02 s) than in restricted arm jumps (-0.17 ± 0.02 s).

The total VGRF was greater ($p = 0.019$) for free (2.38 ± 0.05 BW) than for restricted (2.32 ± 0.05 BW) arm jumps, but the timing of this peak occurred 0.03 s earlier ($p = 0.0004$) in restricted arm jumps (-0.21 ± 0.02 s) than in free arm jumps (-0.18 ± 0.02 s) (Figure 4). The total peak LGRF was 12% greater ($p < 0.0001$) in free (0.84 ± 0.05 BW) than in restricted (0.75 ± 0.05 BW) arm jumps, with the magnitude of LGRF for free arm jumps staying slightly greater in the range of -0.5 to -0.1 s. The time of the total peak LGRF did not differ significantly ($p = 0.5029$) for free (-0.13 ± 0.01 s) and restricted (-0.13 ± 0.01 s) arm jumps.

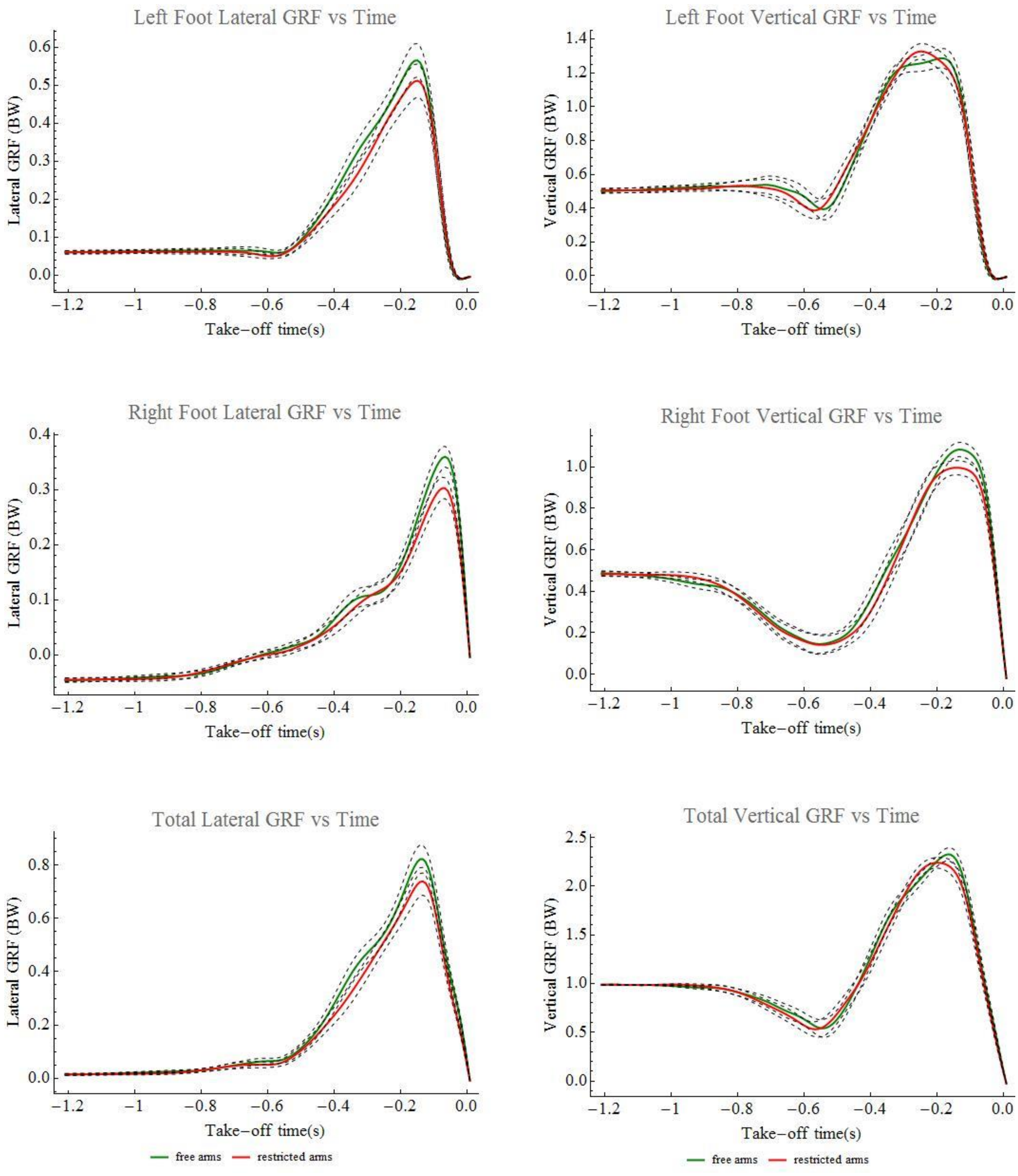

Figure 4: GRF profiles for the last 1.2 s before take-off for both free and restricted arm jumps (mean ± 95% CI)

4.4. Work analysis

The work done by the muscles crossing the lower and upper body joints was calculated for free and restricted arm jumps (Table 2). The total body work was 33% greater ($p < 0.001$) in free arm jumps (511.0 ± 53.6 J) than in restricted arm jumps (384.5 ± 53.6 J). In free arm jumps, significantly more work was performed over restricted arm jumps at the left ankle (82.8 ± 5.3 J compared to 70.8 ± 5.3 J, $p < 0.0001$), the right ankle (83.2 ± 5.5 J compared to 74.2 ± 5.5 J, $p < 0.0001$), the left hip (60.3 ± 9.7 J compared to 38.0 ± 9.7 J, $p = 0.0001$), the right hip (84.7 ± 10.4 J compared to 50.8 ± 10.4 J, $p < 0.0001$), the lower back (52.4 ± 9.9 J compared to 21.6 ± 9.9 J, $p < 0.0001$), the left shoulder (17.4 ± 4.8 J compared to 2.2 ± 4.8 J, $p < 0.0001$), the right shoulder (35.4 ± 5.3 J compared to -3.5 ± 5.3 J, $p < 0.0001$), and the left elbow (16.2 ± 2.4 J compared to 1.1 ± 2.4 J, $p < 0.0001$), with the largest differences (> 30 J) occurring at the lower back, right hip, and right shoulder.

In restricted arm jumps, significantly more work was performed over free arm jumps at the right knee (98.5 ± 16.3 J compared to 80.9 ± 16.3 J, $p = 0.0002$) and right elbow (3.2 ± 12.5 J compared to -24.4 ± 12.5 J, $p = 0.0027$). The work done by muscles crossing the left knee was not significantly different ($p = 0.1455$) for free (21.9 ± 14.3 J) than for restricted (27.4 ± 14.3 J) arm jumps.

Table 2: Work done at different joints (mean ± 95% CI, all work units are Joules (J))

Joint Name	**Free arms**	**Restricted arms**	**p-value**
Left ankle	82.8 ± 5.3	70.8 ± 5.3	<0.0001
Right ankle	83.2 ± 5.5	74.2 ± 5.5	<0.0001
Left knee	21.9 ± 14.3	27.4 ± 14.3	0.1455
Right knee	80.9 ± 16.3	98.5 ± 16.3	0.0002
Left hip	60.3 ± 9.7	38.0 ± 9.7	0.0001
Right hip	84.7 ± 10.4	50.8 ± 10.4	<0.0001
Lower back	52.4 ± 9.9	21.6 ± 9.9	<0.0001
Left shoulder	17.4 ± 4.8	2.2 ± 4.8	<0.0001
Right shoulder	35.4 ± 5.3	-3.5 ± 5.3	<0.0001
Left elbow	16.2 ± 2.4	1.1 ± 2.4	<0.0001
Right elbow	-24.4 ± 12.5	3.2 ± 12.5	0.0027
Total	511.0 ± 53.6	384.5 ± 53.6	<0.0001

Table 3: Work done at lower body (ankle, knee, hip) and upper body (shoulder and elbow) joints (mean ± 95% CI, all work units are Joules (J))

	Free arms	**Restricted arms**	**p-value**
Left lower body joints	165.0 ± 21.2	136.2 ± 21.2	<0.0001
Right lower body joints	248.8 ± 25.2	223.5 ± 25.2	<0.0001
Total lower body joints	413.9 ± 44.9	359.8 ± 44.9	<0.0001
Left upper body joints	33.6 ± 5.8	3.4 ± 5.8	<0.0001
Right upper body joints	11.1 ± 10.3	-0.3 ± 10.3	0.0879
Total upper body joints	44.7 ± 8.4	3.1 ± 8.4	<0.0001

The total work done by the muscles of three main lower body joints was 54.1 J greater ($p < 0.0001$) for free (413.9 ± 44.9 J) than for restricted (359.8 ± 44.9) arm jumps (Table 3), where the hip joints were the main contributors to this difference. The total work done at upper body joints was 41.6 J greater ($p < 0.0001$) in free arm jumps (44.7 ± 8.4 J) compared to restricted arm jumps (3.1 ± 8.4 J), where the right shoulder was the dominant contributor to this difference. The lower back joint did 30.8 J more work ($p < 0.0001$) in free arm jumps (52.4 ± 9.9 J) than in restricted arm jumps (21.6 ± 9.9 J).

4.5 Power analysis of lower back and right hip

Other than the right shoulder, the only two joints to have greater than 30 J increases in work for free arm jumps compared to restricted arm jumps were the lower back and right hip, 30.8 J and 33.8 J increases, respectively. The large increases in work in free arm jumps at those two joints justify further investigation.

4.5.1 Power analysis of lower back

Figure 5 shows the total power at the lower back for the last 1.2 s before take-off. Between about -0.6 s and -0.35 s, power absorption occurred for free and restricted arm jumps. Power generation occurred after -0.35 s at the lower back joints for free arm jumps. Until about -0.25 s the net power generation at free arm jumps was greater compared to restricted arm jumps. Between about -0.25 s and take-off, net power generation for free and restricted arm jumps was not significantly different.

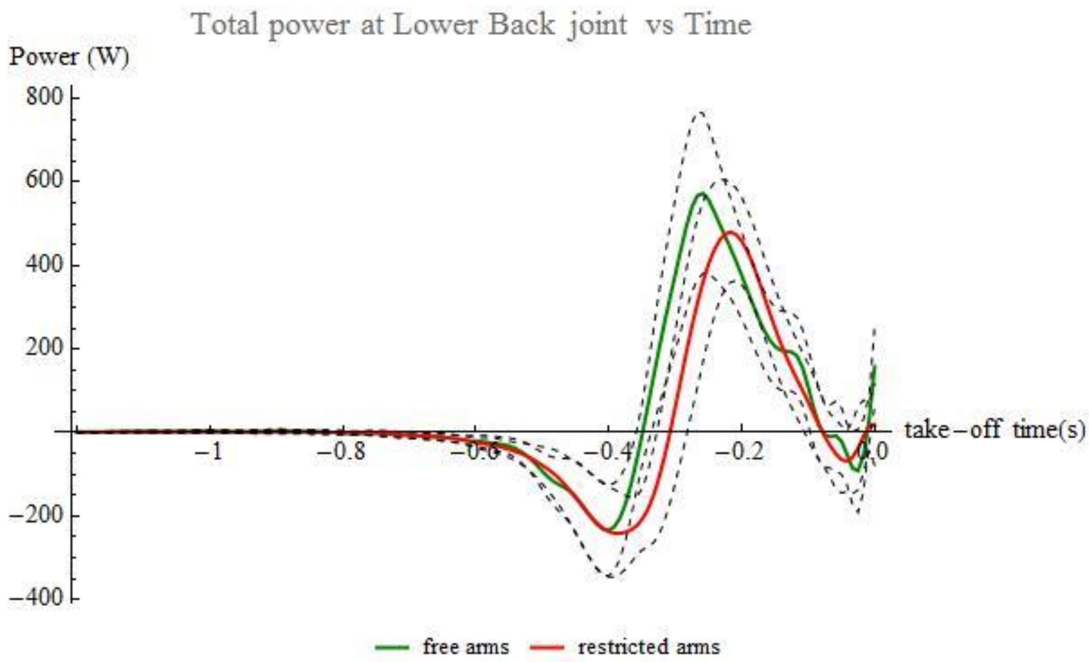

Figure 5: Total power at lower back joint for the last 1.2 s before take-off for free and restricted arm jumps (mean ± 95% CI)

The power due to x, y and z components of the lower back moment in free and restricted arm jumps are shown in Figure 6 expressed in the pelvis anatomical reference frame. It is obvious from the power profiles that most of the power at lower back joints was generated by the flexion/extension moment (about the z-axis) since net power is the sum of the powers generated by the moments about the x (left/right bend), y (left/right rotation), and z axes (equation 23 and 24).

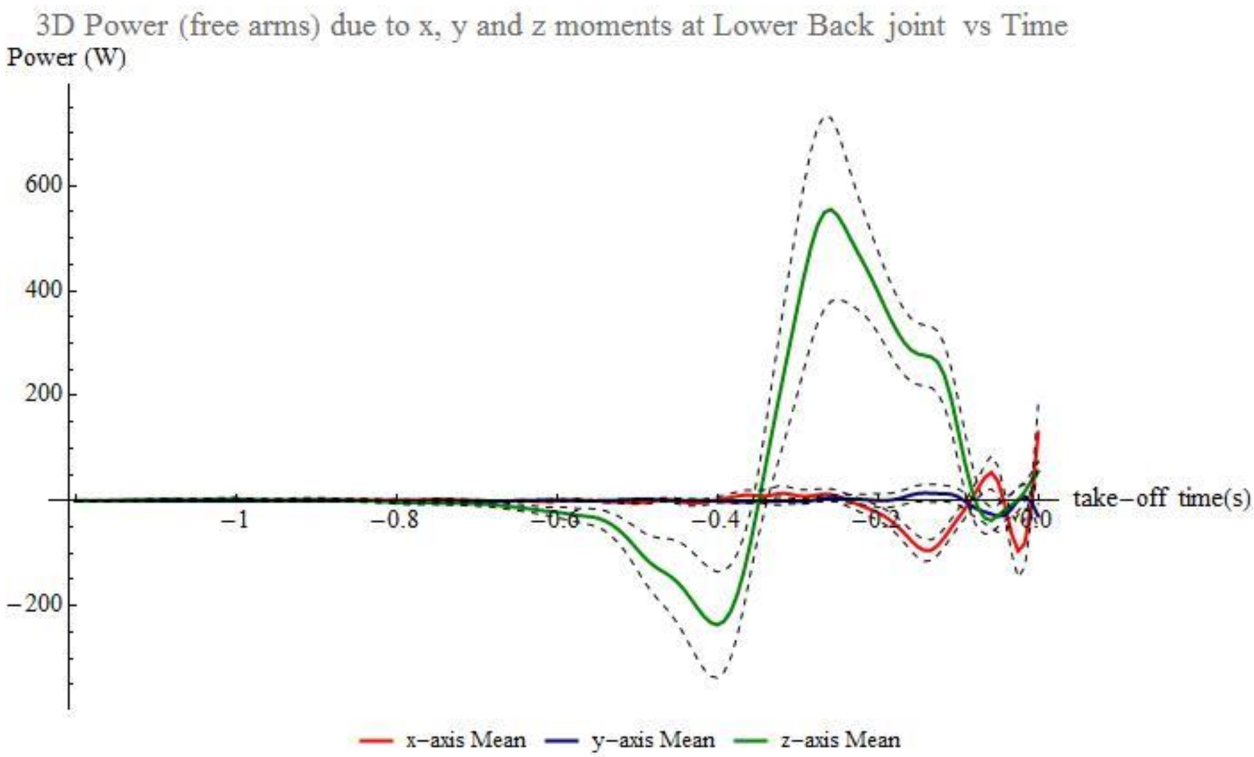

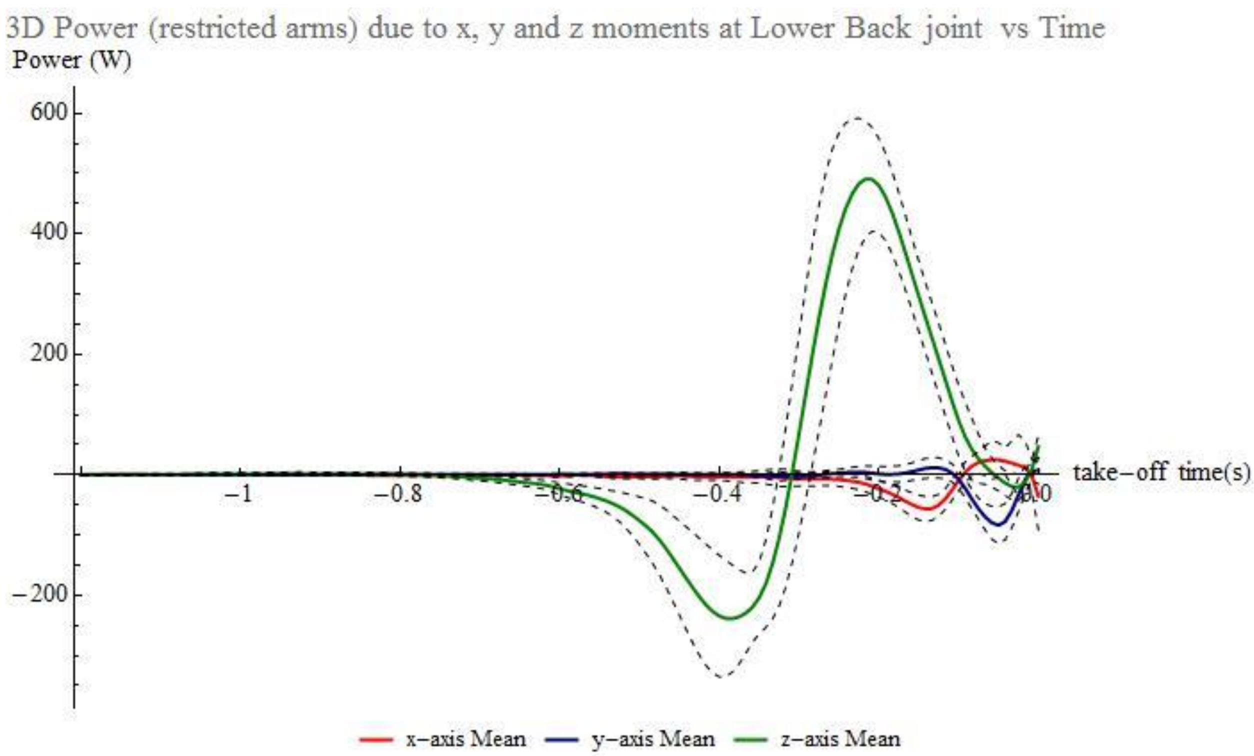

Figure 6: Powers due to moment about z-axis (pelvis anatomical reference frame) at lower back joint for the last 1.2 s before take-off for free and restricted arm jumps (mean ± 95% CI)

Power due to the z-axis moment, the moment about the z-axis, and the angular velocity about the z-axis are examined further (Figure 7) since these were the major contributors in the net lower back joint work for free and restricted arm jumps. Both power profiles for free and restricted arm jumps remained near zero until -0.6 s and varied after -0.6 s. From about -0.4 s to -0.2 s, the power due to the z-axis moment was greater for free arm jumps than for restricted arm jumps. Between about -0.2 s and take-off, the powers for free and restricted arm jumps did not differ significantly.

At the beginning of the jump cycle, the moments about the z-axis at lower back joints for free and restricted jumps were small and increased after -0.8 s. Both moments reached their peaks at about -0.3 s (Figure 7). It is clear from these profiles that the moment for free arm jumps was greater than for restricted arm jumps between about -0.5 s and -0.1 s.

The angular velocity components of the lower back expressed in the pelvis anatomical reference frame are shown for free and restricted arm jumps in Figure 7. From about -1.2 s to - 0.6 s and between about -0.25 s and -0.1 s, the z-axis angular velocity profile was greater for restricted arm jumps than for free arm jumps. Between about -0.5 s and -0.25 s the z-axis angular velocity was greater for free arm jumps. There was no significant difference between the z-axis (flexion/extension) angular velocity profiles for free and restricted arm jumps after -0.1 s to take-off.

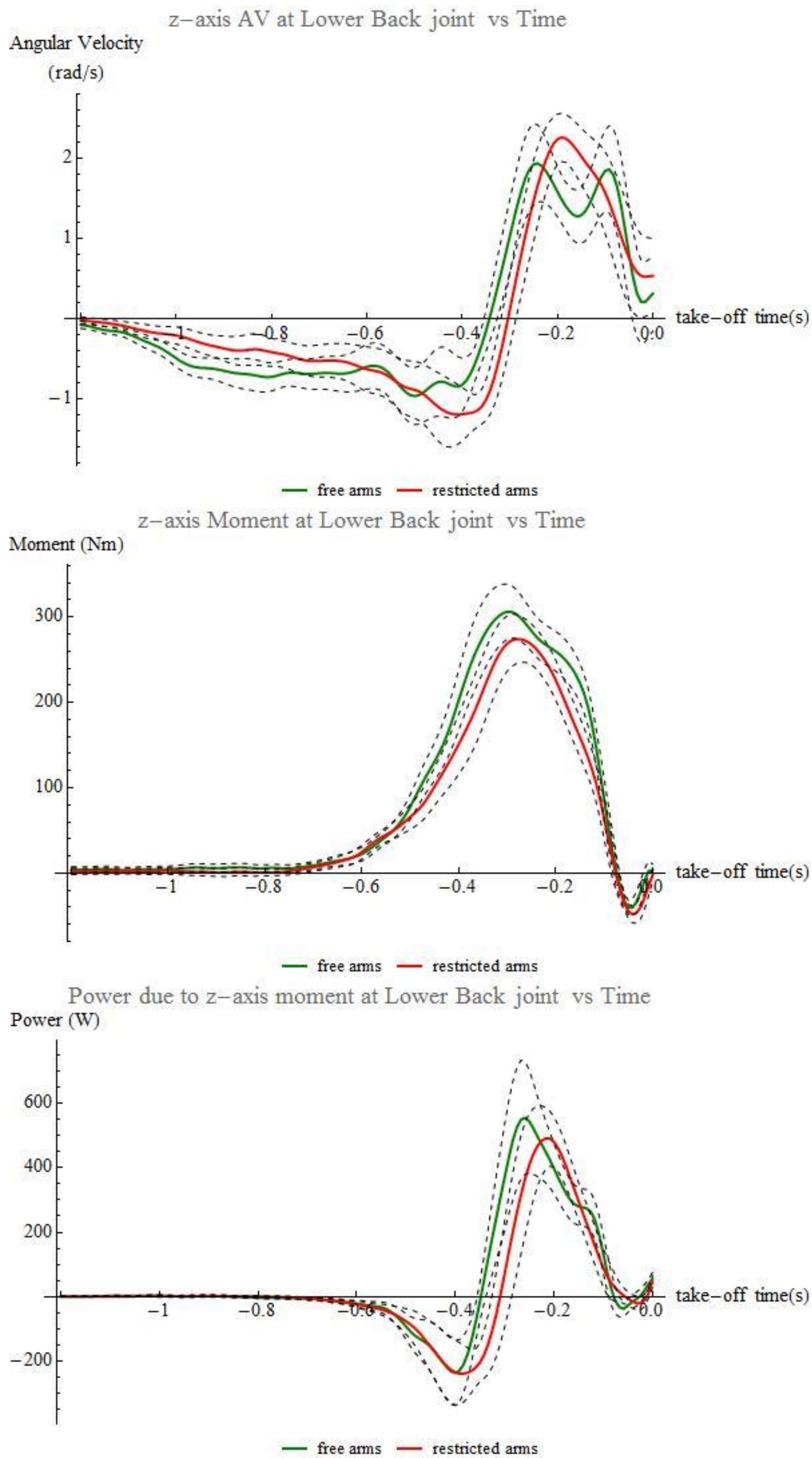

Figure 7: Angular velocity, moment and power about z-axis (pelvis anatomical reference frame) at lower back for the last 1.2 s before take-off for free and restricted arm jumps (mean ± 95% CI)

4.5.2 Power analysis of right hip

Figure 8 shows the total power generation and absorption at the right hip for the last 1.2 s before take-off. Between -0.6 s and -0.4 s, power absorption occurred for free and restricted arm jumps. After -0.4 s power generation happened until about -0.05 s. Between about -0.15 s and - 0.05 s, the net power generation at the right hip was greater in free arm jumps than in restricted arm jumps.

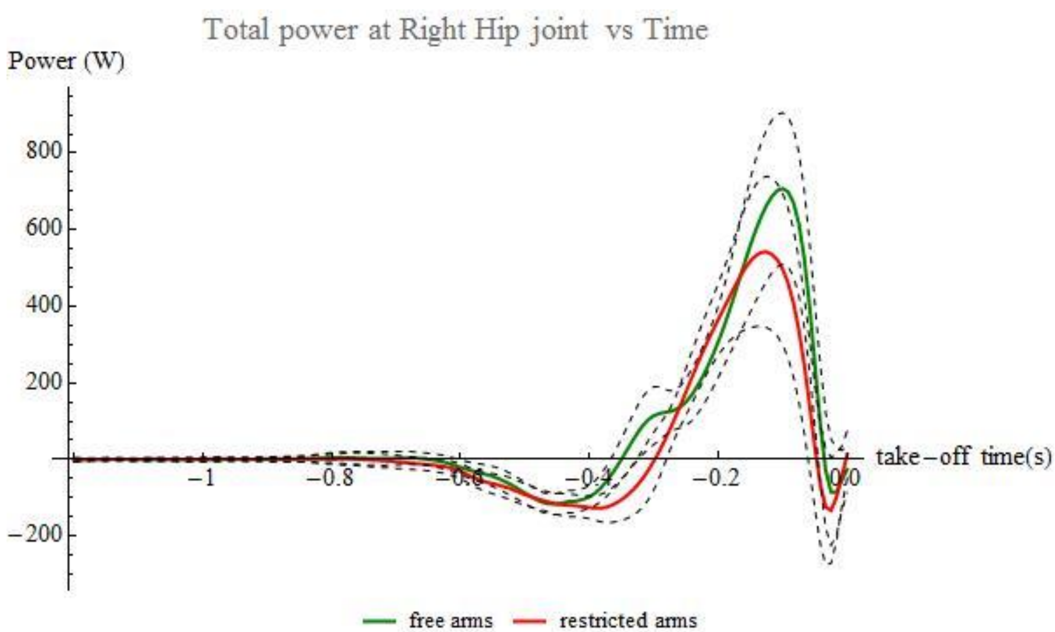

Figure 8: Total power at right hip joint for the last 1.2 s before take-off for free and restricted arm jumps (mean ± 95% CI)

The power due to x, y and z components of the right hip moment in free and restricted arm jumps are shown in Figure 9 expressed in the thigh anatomical reference frame. Similar to the lower back joint, most of the power at the right hip was generated by the flexion/extension moment (about the z-axis). There was also some power generation and absorption by the y (internal/external rotation) and x (adduction/abduction) components of the moment. As power due to the moment about z-axis was the major contributor to total power and work for the right hip, the moment and angular velocity about the z-axis are examined here. Since power generation due to the moment about x and y axes was very small (Figure 9) for free and restricted arm jumps, the power profiles (Figure 10) for the moment about z axis is almost similar to the net power profiles (Figure 8) for right hip.

The moments about z axis at the hip joint remained near to zero for free and restricted arm jumps at the beginning of jump and increased after -0.6 s (Figure 10). Between about -0.6 s and -0.1 s the z-axis moment was greater for free arm jumps compared to restricted arm jumps.

There was no significant difference between the z-axis angular velocity profiles (Figure 10) and both almost traced each other between about -1.2 s and -0.1 s. After -0.1 s, the z-axis angular velocity profile for free arm jumps stayed slightly greater than for restricted arm jumps until take-off.

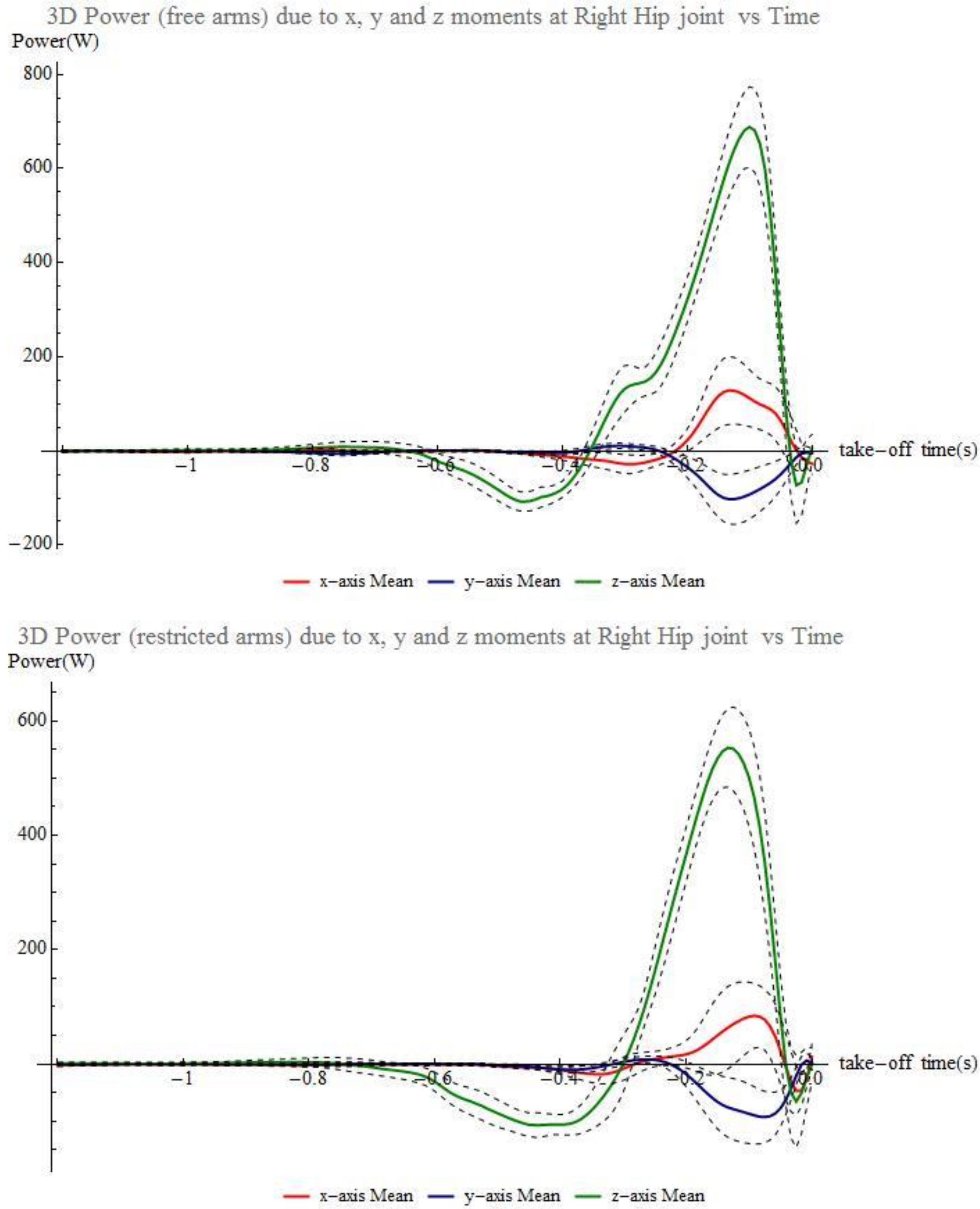

Figure 9: Powers due to moment about z-axis (thigh anatomical reference frame) at right hip joint for the last 1.2 s before take-off for free and restricted arm jumps (mean ± 95% CI)

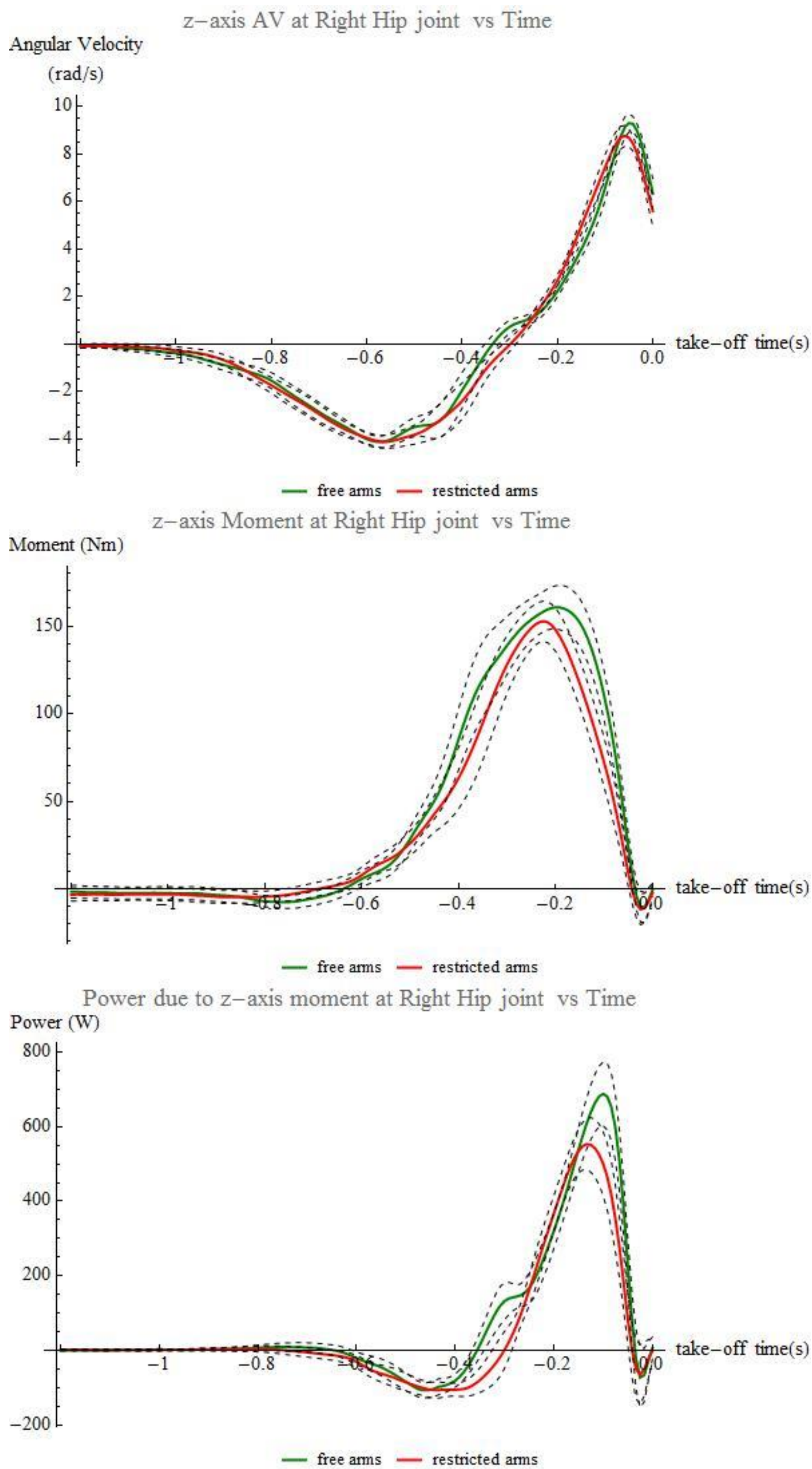

Figure 10: Angular velocity, moment and power about z-axis (thigh anatomical reference frame) at right hip for the last 1.2 s before take-off for free and restricted arm jumps (mean ± 95% CI)

5 Discussion

Several studies showed that the arm swing has a positive effect on standing vertical and forward jump performance. Investigators also demonstrated the benefits of the arm movement on jump distance and explored the mechanisms underlying the improved performance. In addition, researchers have analyzed the motor coordination of lower extremity movement in lateral jumping in a few studies. However, before the present study, no studies had examined standing two-leg lateral jumps with two leg landing or the role of arm movement on lateral jump performance. The purpose of this study was to study the effects of arm swing on jumping performance of two-leg lateral jumps and to investigate the mechanisms underlying any performance change.

In this study, participants jumped 29% (35.6 cm) farther in free arm jumps over restricted arm jumps. Of the 35.6 cm improvement, 29% (10.2 cm) was due to the increase in the lateral and vertical CG position relative to the right foot at take-off, 15% (5.4 cm) was due to the position of the CG relative to the left foot at landing, and 56% (20.0 cm) was due to the increase in CG velocity at take-off.

The present study is the first to explore the arm swing effect on lateral jump performance, so arm contributions to lateral jump performance were compared to similar standing long jump and vertical jump studies. In previous standing long jump studies, jump performance improvement due to arm motion was 21% (36 cm) (Ashby and Heegaard, 2002) and 15% (31 cm) (Hara et al., 2008). This present study found a 29% (35.6 cm) increase in jump performance due to allowed arm motion. This study also found a 7.2 cm increase in the lateral position of the CG with respect to the right foot and a 2.4 cm increase in the CG vertical position due to arm movement. These results are comparable to the 8 cm and 2 cm increase in CG horizontal and vertical directions, respectively, reported in a standing long jump study (Ashby and Heegaard, 2002). In comparable vertical jump studies, the increase in CG height at take-off was reported as 4.5 cm (Harman et al., 1990), 6.1 cm (Feltner et al., 1999), 2.4 cm (Lees et al., 2004), and 5 cm (Blache et al., 2013).

The take-off velocity increase due to free arm motion was found to be 13%, which is similar to the reported 13% (Ashby and Heegaard, 2002) and 11.8% (Hara et al., 2008) increases in take-off velocity in standing long jump studies, and the 10% (Harman et al., 1990; Feltner et al., 1999), 12.7% (Luhtanen and Komi, 1978), and 8.9% (Lees et al., 2004) reported in vertical jump studies. The calculated take-off angle 39.6º in free arm jumps is also very close to the 38.6º (Ashby and Heegaard, 2002), 37.5º (Aguado et al., 1997), and 32.2º (Hara et al., 2008) of standing free arm long jump studies. The total peak vertical and lateral GRF values of 2.38 BW and 0.84 BW, respectively, in free arm jumps, are also in good agreement with previously reported vertical (2.27-2.31 BW) and horizontal (0.63-0.88 BW) GRF values from standing forward jump studies (Aguado et al., 1997; Ashby and Heegaard, 2002; Filush, 2012).

Since no previous study has reported on joint work during standing lateral jumps, joint work analysis was compared to similar standing long jump studies (Table 4). Joint work values in free arm jumps for the present study are compared with the findings from previous standing long jump investigations.

Table 4: Work comparison at different joints for present lateral jump study with previous standing long jump studies (Hara et al., 2008; Filush, 2012), all work units are Joules (J).

	Present study, 3D	**Hara, 2D**	**Filush, 2D**
Work done at Ankle	166	140	226
Work done at Knee	102.8	44	82
Work done at Hip	145	361	167
Work done at Lower Back	52.4	NA	NA
Work done at Shoulder	52.8	5	94
Work done at Elbow	-8.2	17	-16.9
Total Body Work	511	583	553

In both lateral and forward standing free arm jumps, ankle, knee, hip joints are the dominant locations for energy generation. Work done at lower joints differs with results from all the compared investigations. In the present 3D study, one extra joint (lower back) was considered, which was missing in 2D models of the compared studies. The presence of the lower back joint in the present study may explain lower work values found at the hip joint. There are differences in the work values at shoulder and elbow joints among the studies. The ankle work done, and total body work done in the present study also differ with results from standing long jump studies. These variations could be due to the differences in segmental movements between these two types of jumps since the lateral jump movement is not same as forward jump movement. Given that the standing long jump distances are much greater than lateral jump distances, the total body work values should be much greater in standing forward jumps compared to lateral jumps. The work differences at the joints could also be due to differences in the athletic and physical ability of the considered participants for the respective jump studies.

In a previous standing long jump study, the total work improvement due to free arm movement was found to be 69 J (Hara et al., 2008), which is less than the present findings of 126.5 J. The total lower joint work improvement of 54.1 J due to free arm motion in the present study is close to the 42 J previously reported by Hara et al. (2008). In the present investigation, muscles crossing the upper body joints did 41.6 J extra net work due to free arm motion. This extra upper limb work was close to the previously reported work improvement of 31 J (Hara et al., 2008) in standing long jumps. The work done at left and right shoulder joints was 15.1 J and 39 J greater respectively in free arm lateral jumps compared to restricted arm lateral jumps. The work at left elbow was also 15.1 J greater in free arm jumps compared to restricted arm jumps. But, -24.4 J energy was absorbed at the right elbow in free arm jumps, which was 27.6 J less than in restricted arm jumps.

In the present study, arm motion improved jump performance by increasing the total work done by 33% (126.5 J). 43% (54.1 J) of that extra work due to free arm movement came from the lower body joints, 33% (41.6 J) came from the upper body joints, and 24% (30.8 J) came from the lower back. In previous standing long jump studies, it was reported that additional energy imparted to the system due to the work done at upper extremity joints was the largest factor in increasing the take-off velocity as well as the jump performance in free arm jumps (Harman et al. 1990, Lees et al., 2004, Ashby and Delp, 2006, Cheng et al., 2008). In the present study, the total amount of additional work 41.6 J at the shoulder and elbow joints played an important role in increasing the CG velocity at take-off by imparting extra energy to the system.

In previous vertical jump studies, arm swing was found to enhance the ability of lower body extensor muscles to produce larger forces due to decreased muscle shortening (Feltner et al., 1999; Feltner et al., 2004; Hara et al., 2006 and Cheng et al., 2008). Standing long jump simulations by Ashby and Delp (2006) also demonstrated work improvement in free arm standing long jumps due to torque augmentation allowed by lower extension velocities at the hip and ankle joints. In the present study, arm swing could have had a similar effect on the ankles, hips, and lower back since work improvement was evident at these joints due to free arm motion. At about -0.4 s to - 0.2 s power due to the moment about z-axis at the lower back joint in free arm jumps was greater than the restricted arm jumps (Figure 7). The moment about z-axis at the lower back joint was also greater in free arm jumps during this time (Figure 7). However, this increased moment about the z-axis in free arm jumps was caused when the z-axis angular velocity in free arm jumps was greater compared to restricted arm jumps (Figure 7). Similarly, at the right hip joint, a greater power was generated due to greater moment about z-axis in free arm jumps compared to restricted arm jumps between about -0.15 s and take-off. There was no significant difference in z-axis angular velocities for free and restricted arm jumps during this time before take-off. Thus, it can be concluded that the greater moment at the lower back and right hip joints was not due to the reduced angular velocities of the extensor muscles crossing these two joints as a result of arm motion.

The increased moments in free arm jumps compared to restricted arm jumps at the lower back and right hip could be generated due to changes in muscle activations, muscle lengths, and moment arms. Differences in the lower back and right hip joint angles would result in differences in the lengths and moment arms of the associated extensor muscles. Further investigations are needed to quantify the net effect of these differences in muscle moments, powers, and work generation. The shape of the right hip and lower back moment profiles for free arm and restricted arm jumps in the present study suggests that these types of jumps may have had differences in muscle activations. The timing of muscle activations during the jump could explain the greater joint moments and powers observed. Future electromyography (EMG) or simulation studies could provide insight into muscle activation patterns and relative degrees of force generation.

The timing of the vertical GRF profiles (Figure 4) suggests that the jumpers may have been holding back just before take-off in restricted arm jumps. The peak value of the vertical GRF occurred 0.03 s earlier ($p = 0.0004$) in restricted arm jumps and trailed off sooner before take-off, which indicates that the participants may not have used all the available muscle force during this portion of take-off phase. This evidence supports the “hold back” theory, which suggests that when arms are restrained, the jumper may limit activation of the extensor muscles during the propulsive phase to eliminate rotation that would preclude proper landing (Ashby and Heegaard, 2002). However, without knowing the actual neural activations of the muscles, whether or not the participants were holding back in restricted arm lateral jumps cannot be determined. Future computer simulation studies that estimate activations could provide insight into the motor coordination principles of the standing lateral jump and the mechanisms of enhanced jump performance due to arm swing.

During the data collection, participants were asked to jump to the right side. Jump performance could vary if the participants were asked to jump according to their dominant side (left or right). It is also possible that the presence of the reflective markers affected the manner in which the participants used their arms in free arm jumps. Training the participants while the markers are on could make a difference in this kind of jump study.

The sample size (six participants) for this study is also a limitation because of the inability to generalize to the larger population. Collecting data on a greater number of participants could strengthen the conclusions reached in this study. In this study, inverse dynamics which has some inherent limitations was used to calculate the joint moments. The assumptions of this method are not always valid. Some joints may have friction and mass distribution in the segments can vary. Estimation of the joint center is prone to error because of the errors resulting from soft tissue artifacts. The accuracy of position measurement by reflective markers is limited by marker motion on the skin and at the skin-bone interface and by the algorithms used to fill the gaps in the data due to missing markers. These errors are exacerbated by numerical differentiation to get velocities and accelerations and are propagated through the successive segments in “bottom-up” and “top-down” inverse dynamics calculations, which limits the accuracy of the calculated moment, power, and work. Future investigations might be done using alternate calculation strategies to minimize these errors.

6 Conclusion

Arm swing generally improves the jump performance in vertical and standing long jump movement, which was previously shown in many studies. In this study, the role of arm movement on standing two-leg lateral jump performance was examined.

This study found that jump performance was improved by 29% due to free arm swing in standing two-leg lateral jumps. The jump performance improvement was due to the increase in take-off velocity, and the change in lateral and vertical CG position at take-off and touchdown in free arm jumps. In free arm jump, 33% additional work was done which increased the take-off velocity and improved the CG position at take-off. Some upper body (shoulders), lower body (ankles and hips), and lower back joints did greater work to increase the total body work in free arm jumps compared to restricted arm jumps. Total work at upper body joints (shoulders and elbows) was greater in free arm jumps. The extra energy imparted to the system by the upper body joints was used to increase jump performance. The work differences were greatest (>30 J) at the lower back, right hip, and right shoulder joints in free arm jumps. The mechanisms underlying these work improvements were investigated by examining the "joint torque augmentation" theory. No evidence of joint torque augmentation was found to explain the work improvement at the lower back and right hip joints due to slower joint extension velocities. The work improvement at the lower back and right hip might have been a result of differences in muscular activation, muscle fiber lengths, moment arms, or some combination of all three. Future studies are required to more completely understand the mechanisms enabling this work improvement.

Appendices

Appendix A

Following are descriptions of the anatomical coordinates systems used in the 3D model of Hickox, et al., (2014) jump study which is adapted from ISB recommendations

Here,

-All x-axes point in the anterior direction

-All y-axes are along the long axis of the segment and point in the proximal direction

-All z-axes point towards the right side of the subject.

Note: Abbreviations used in this summary are consistent with Marker Set Table

Foot Coordinate System – origin at HEE

x-axis: HEE to midpoint between MT1 and MT5

y-axis: perpendicular to plane with MT1, MT5, and HEE

z-axis: perpendicular to x-axis and y-axis

Shank Coordinate System – origin at KJC

x-axis: AJC to KJC

y-axis: perpendicular to plane containing AJC, KJC, and FBH

z-axis: perpendicular to x-axis and y-axis

Thigh Coordinate System – origin at HJC

x-axis: KJC to HJC

y-axis: perpendicular to plane containing HJC, LKNE, and MKNE

z-axis: perpendicular to x-axis and y-axis

Pelvis Coordinate System – origin at midpoint between LHJC and RHJC

x-axis: LBJC to midpoint between LHJC and RHJC

y-axis: perpendicular to the plane containing LHJC, RHJC, and LBJC z-axis: perpendicular to x-axis and y-axis

Trunk (Thorax) Coordinate System – origin at the midpoint between CLAV and C7

x-axis: LBJC to midpoint between CLAV and C7

y-axis: perpendicular to plane with CLAV, C7, and LBJC

z-axis: perpendicular to x-axis and y-axis

Upper Arm Coordinate System – origin at SJC

x-axis: EJC to SJC

y-axis: perpendicular to plane containing LE, ME, and SJC

z-axis: perpendicular to x-axis and y-axis

Forearm Coordinate System – origin at WJC

x-axis: WJC to EJC

y-axis: perpendicular to plane containing ME, LE, and WJC

z-axis: perpendicular to x-axis and y-axis

Appendix B

Marker set for 3D model (modified from marker set used in Hickox (2014)).

Marker Name	Location
Left Lower Extremity	
LTHI1	Left Thigh 1
LTHI2	Left Thigh 2
LTHI3	Left Thigh 3
LLKNE	Left Lateral Femoral Epicondyle
LMKNE	Left Medial Femoral Epicondyle
LSHN	Left Anterior Crest of Tibia
LTUB	Left Tibial Tuberosity
LFBH	Left Fibular Head
LLML	Left Lateral Malleolus
LMLL	Left Medial Malleolus
LHEE	Left Heel
LMT1	Left Head of 1st Metatarsal
LMT5	Left Head of 5th Metatarsal
Right Lower Extremity	
RTHI1	Right Thigh 1
RTHI2	Right Thigh 2
RTHI3	Right Thigh 3
RLKNE	Right Lateral Femoral Epicondyle
RMKNE	Right Medial Femoral Epicondyle
RSHN	Right Anterior Crest of Tibia
RTUB	Right Tibial Tuberosity
RFBH	Right Fibular Head
RLML	Right Lateral Malleolus
RMLL	Right Medial Malleolus
RHEE	Right Heel
RMT1	Right Head of 1st Metatarsal
RMT5	Right Head of 5th Metatarsal
Pelvis	
LASI	Left Anterior Superior Iliac Spine
RASI	Right Anterior Superior Iliac Spine
LPSI	Left Posterior Superior Iliac Spine
RPSI	Right Posterior Superior Iliac Spine
Trunk	
CLAV	Jugular Notch
STRN	Xyphoid Process
T8	Mid-lower Back

C7	7th Cervical Vertebra
LACR	Left Acromion Process
RACR	Right Acromion Process
RBAK	Right Shoulder Blade
Left Upper Extremity	
LUS	Left Ulnar Styloid
LRS	Left Radial Styloid
LFRM	Left Forearm (Lateral Side)
LLE	Left Lateral Epicondyle
LME	Left Medial Epicondyle
LUA1	Left Upper Arm 1
LUA2	Left Upper Arm 2
LUA3	Left Upper Arm 3
Right Upper Extremity	
RUS	Right Ulnar Styloid
RRS	Right Radial Styloid
RFRM	Right Forearm (Lateral Side)
RLE	Right Lateral Epicondyle
RME	Right Medial Epicondyle
RUA1	Right Upper Arm 1
RUA2	Right Upper Arm 2
RUA3	Right Upper Arm 3
Total: 55 markers	

Table: The sign convention (Hickox et al., 2014)

Joint	Motion about x- axis (-/+)	Motion about y -axis (-/+)	Motion about z -axis (-/+)
Ankle	Inversion Eversion	Internal/External Rotation	Dorsiflexion/Plantarflexion
Knee	Varus/Valgus	Internal/External Rotation	Flexion/Extension
Hip	Adduction/Abduction	Internal/External Rotation	Flexion/Extension
Lower Back	Left/Right Bend (of upper body)	Left/Right Rotation (of upper body)	Flexion/Extension
Shoulder	Adduction/Abduction	Internal/External Rotation	Flexion/Extension
Elbow	Adduction/Abduction	Internal/External Rotation	Flexion/Extension

Appendix C

The XYZ Euler rotation angles used in Hickox, (2014) model were chosen in the following order:

α= Rotation about the z-axis (flexion/extension or dorsiflexion/plantarflexion)

β= Rotation about the x-axis (abduction/adduction, varus/valgus, inversion/eversion)

γ= Rotation about the y-axis (internal/external rotation)

The rotation matrix for the joint angles was determined by sing following equation

$$R_{joint} = R_{xyz} = [R_{z''}][R_{y'}][R_x] \quad \text{(C1)}$$

The individual rotation matrices about each of the axis are

$$R_x = \begin{bmatrix} 1 & 0 & 0 \\ 0 & \cos\beta & \sin\beta \\ 0 & -\sin\beta & \cos\beta \end{bmatrix} \quad \text{(C2)}$$

$$R_y = \begin{bmatrix} \cos\gamma & 0 & -\sin\gamma \\ 0 & 1 & 0 \\ \sin\gamma & 0 & \cos\gamma \end{bmatrix} \quad \text{(C3)}$$

$$R_z = \begin{bmatrix} \cos\alpha & \sin\alpha & 0 \\ -\sin\alpha & \cos\alpha & 0 \\ 0 & 0 & 1 \end{bmatrix} \quad \text{(C4)}$$

Using equation A1 and multiplying individual rotation matrices per this, the following joint rotation matrix can be form

$$R_{joint} = \begin{bmatrix} \cos\alpha\cos\gamma & \cos\beta\sin\alpha + \cos\alpha\sin\beta\sin\gamma & \sin\alpha\sin\beta - \cos\alpha\cos\beta\sin\gamma \\ -\cos\gamma\sin\alpha & \cos\alpha\cos\beta - \sin\alpha\sin\beta\sin\gamma & \cos\alpha\sin\beta + \cos\beta\sin\alpha\sin\gamma \\ \sin\gamma & -\cos\gamma\sin\beta & \cos\beta\cos\gamma \end{bmatrix} \quad \text{(C5)}$$

The A5 equation will be used to compare along with determined joint rotation matrix to calculate Euler rotation angles α, β and γ respectively.

$$\gamma = \sin^{-1} R_{31} \quad \text{(C6)}$$

$$\beta = \tan^{-1}\left(\frac{R_{32}}{-\cos(\gamma)} \Big/ \frac{R_{33}}{\cos(\gamma)} \right) \quad \text{(C7)}$$

$$\alpha = \tan^{-1}\left(\frac{R_{21}}{-\cos(\gamma)} \Big/ \frac{R_{11}}{\cos(\gamma)} \right) \quad \text{(C8)}$$

Appendix D

GRAND VALLEY STATE UNIVERSITY
www.gvsu.edu

Volunteer Survey

Age (Years and months): _____________ Height: _________ Weight:_________

1) How often do you participate in any sort of physical activity

   a) < 1 time per week
   b) 1 – 2 times per week
   c) 3 – 5 times per week
   d) > 5 times per week

2) What is the typical duration of your physical activity?

   a) < 20 minutes
   b) 20 – 40 minutes
   c) 40 – 60 minutes
   d) > 60 minutes

3) What is the typical level of exertion during your physical activity?

   a) mild
   b) moderate
   c) strenuous

4) How often is jumping involved in your physical activity?

   a) I don’t participate in any physical activity
   b) Rarely
   c) Moderately often
   d) Frequently

5) Have you ever suffered injury to your ankles, knees, hips, shoulders, elbows, back, or neck?

   Yes No

6) If 5) was answered “Yes,” please describe the nature of your injury/injuries.

7) Are you still experiencing any negative effects from this/these injury/injuries?

   Yes No

8) Is your current physical activity limited in any way by a physician?

   Yes No

9) If 8) was answered “Yes,” please describe the nature of this limitation.

References

Aguado, X., Izquierdo, M., Montesinos, J.L., 1997. Kinematic and kinetic factors related to the standing long jump performance. Journal of Human Movement Studies 32, 156-169.

Aizawa, J., Ohji S., Koga, H., Masuda, T., Yagishita, K., 2016. Correlations between sagittal plane kinematics and landing impact force during single-leg lateral jump-landings. J. Phys. Ther. Sci. 28: 2316–2321.

Ashby, B.M., Heegaard, J.H., 2002. Role of arm motion in the standing long jump. Journal of Biomechanics 35, 1631-1637.

Ashby B.M., 2004. Coordination of upper and lower limbs in the standing long jump: kinematics, dynamics, and optimal control (Ph.D. dissertation). Stanford University, Stanford, CA.

Ashby, B. M., & Delp, S. L. 2006. Optimal control simulations reveal mechanisms by which arm movement improves standing long jump performance. Journal of Biomechanics, 39(9), 1726-1734.

Ashby, B.M., Vlietstra, N., Hickox, L.J., and Alderink, G.J., 2015. Methods for Full Body Inverse Dynamics Analysis of Standing Long Jump 39th Meeting of the American Society of Biomechanics, August 5–8.

Blache Y, Monteil K., 2013. Effect of arm swing on effective energy during vertical jumping: Experimental and simulation study. Scandinavian Journal of Meicine and Science in Sports, 23: e121–e129.

Cheng, K., Wang, C.H., Chen, H.C., Wu, C.D., Chiu, H.T., 2008. The mechanisms that enable arm motion to enhance vertical jump performance – a simulation study. Journal of Biomechanics 41, 1857-1854.

Dapena, J., 1993. Biomechanical studies in the high jump and implications for coaching. Modern Athlete and Coach 31 (4), 7–12.

Domire, Z.J., Challis, J.H., 2010. An induced energy analysis to determine the mechanism for performance enhancement as a result of arm swing during jumping. Sports Biomechanics March 2010; 9(1): 38–46.

de Leva, P., 1996. Adjustments to Zatsiorsky-Seluyanov's segment inertia parameters. Journal of Biomechanics 29, 1223-1230.

Ehrig, R.M., Taylor, W.R., Duda, G.N., Heller, M.O., 2006. A survey of formal methods for determining the centre of rotation of ball joints. Journal of Biomechanics 39, 2798-2809.

Filush, A. and Ashby, B.M., 2012. Effect of Using Hand Weights on Performance in the Standing Long Jump, Biomedical Engineering Society Annual Meeting, Atlanta, GA, October 24–27.

Filush, A., 2012. Effect of Using Hand Weights on Performance in the Standing Long Jump (Master's thesis). Grand Valley State University, Allendale, MI.

Feltner, M.E., Fraschetti, D.J., Crisp, R.J., 1999. Upper extremity augmentation of lower extremity kinetics during countermovement vertical jumps. Journal of Sports Sciences 17, 449–466.

Feltner, M.E., Bishop E.J., Perez C.M., 2004. Segmental and Kinetic Contributions in Vertical Jumps Performed With and Without an Arm Swing. Research Quarterly for Exercise and Sport, Physical Education, Recreation and Dance, Vol. 75, No. 3, pp. 216-230.

Harman, E.A., Rosenstein, M.T., Frykman, P.N., Rosenstein, R.M., 1990. The effect of arms and countermovement on vertical jumping. Medicine and Science in Sports and Exercise 22, 825–833.

Hara, M., Shibayama, A., Arakawa, H., Fukashiro, H., 2008. Effect of arm swing direction on forward and backward jump performance. Journal of Biomechanics 41, 2806–2815.

Hara, M., Shibayama A., Takeshita, D., Fukashiro, S., 2006. The effect of arm swing on lower extremities in vertical jumping. Journal of Biomechanics 39 (2006) 2503–2511.

Hewit, J.K., Cronin, J.B., Humea, PA., 2012a. Asymmetry in multi-directional jumping tasks. Physical Therapy in Sport 13, 238-242.

Hewit, J., Cronin, J., Hume, P.,2012b. Multidirectional Leg Asymmetry Assessment in Sport. Strength & Conditioning Journal, Volume 34 - Issue 1 - pp 82-86.

Hickox, L., 2014. Exploration of the Validity of the Two-Dimensional Sagittal Plane Standing Long Jump Model (Master's thesis). Grand Valley State University, Allendale, MI.

Hickox, L.J., Ashby, B.M., and Alderink, G.J., 2016. Exploration of the Validity of the Two-Dimensional Sagittal Plane Assumption in Modeling the Standing Long Jump, Journal of Biomechanics, Vol. 49, pp. 1085–1093.

Lees, A., Vanrenterghem, J., Clercq, D.D, 2007. The energetics and benefit of an arm swing in submaximal and maximal vertical jump performance. Journal of Sports Sciences, 24:1, 51-57

Lees, A., Vanrenterghem, J., de Clercq, D., 2004. Understanding how an arm swing enhances performance in the vertical jump. Journal of Biomechanics 37, 1929-1940.

Lee, Y.M., Lee, H.J., 2012. Effects of different jump-landing directions on sagittal plane kinematics, kinetics and energy dissipation at lower extremity joints. 30th Annual Conference of Biomechanics in Sports – Melbourne

Lees, A. and Barton, G, 1996. The interpretation of relative momentum data to assess the contribution of the free limbs to the generation of vertical velocity in sports activities. Journal of Sports Sciences, 14:503–511.

Lockie, R.G., Schultz, A.B., Luczo, T.M., Callaghan, S.J., Jeffriess, M.D., 2013. Effect of unilateral dynamic stability on lateral jump performance in team sport athletes. Serbian Journal of Sports Sciences, Vol. 7 Issue 4, p159-166. 8p.

Lockie, R.G., Jalilvand, F., Jordan, C.A., Callaghan, S.J., Jeffriess, M.D., Luczo, T.M., Schultz, A.B., 2015. The Relationship between Unilateral Dynamic Stability and Multidirectional Jump Performance in Team Sport Athletes, vol. XXIV, no. 5-6, 321-344

Luhtanen, P., Komi, P.V., 1978. Segmental Contribution of Force in Vertical Jump. Europ. J. Appl. Physiol. 38, 181-188 (1978)

Mackala, K., Stodólka, J., Siemienski, A., Coh, M., 2013. Biomechanical analysis of standing long jump from varying positions. Journal of Strength and Conditioning Research 27, 2674–2684.

Meylan, C. M. P., Nosaka, K., Green, J. and Cronin, J. B., 2010a. Temporal and kinetic analysis of unilateral jumping in the vertical, horizontal, and lateral directions. Journal of Sports Sciences, 10.1080/02640411003628048

Meylan, C.M.P., Nosaka, K., Green, J.P., and Cronin, J.B., 2010b. Variability and influence of eccentric kinematics on unilateral vertical, horizontal, and lateral countermovement jump performance. Journal of Strength and Conditioning Research. 24(3): 840-845.

Mornieux, G., Gehring, D., Tokuno, C., Gollhofer, A., Taube, W., 2014. Changes in leg kinematics in response to unpredictability in lateral jump execution. European Journal of Sport Science, Vol. 14, No. 7, 678–685.

Nagano, A., Komura, T., Fukashiro, S., 2007. Optimal coordination of maximal-effort horizontal and vertical jump motions – a computer simulation study. Biomedical Engineering Online 6-20.

Payne, A.H., Slater, W.J., Telford, T., 1968. The use of a force platform in the study of athletic activities. A preliminary investigation. Ergonomics 11, 123–143.

Ren, L., Jones, R.K., Howard, D., 2008. Whole body inverse dynamics over a complete gait cycle based only on measured kinematics. Journal of Biomechanics 41, 2750-2759.

Shetty, A.B., Etnyre B.R., 1989. Contribution of Arm Movement to the Force Components of a Maximum Vertical Jump. The Journal of Orthopedics and Sports Physical Therapy. 0190-6011/89/1105-0198$02.00/0

Sinsurin, K., Vachalathiti, R., Jalayondeja, W., Limroongreungrat, W., 2013. Altered Peak Knee Valgus during Jump-Landing among Various Directions in Basketball and Volleyball Athletes. Asian Journal of Sports Medicine, Volume 4, 195-200.

Vlietstra, N., 2014. Comparing Methods for Full Body Inverse Dynamics Analysis of a Standing Long Jump (Master's thesis). Grand Valley State University, Allendale, MI.

Wakai, M., Linthorne, N.P., 2005. Optimum take-off angle in the standing long jump. Human Movement Science 24, 81-96.

Winter, D., 2009. Biomechanics and motor control of human movement, fourth edition. John Wiley and Sons, Waterloo, Ontario, Canada.

Wu, W., Wu, J., Lin, H., & Wang, G. (2003). Biomechanical analysis of the standing long jump. Biomedical Engineering: Applications, Basis and Communications, 15(05), 186-192.

Wu, G., Siegler, S., Allard, P., Kirtley, C., Leardini, A., Rosenbaum, D., Whittle, M., D'Lima, D.D., Cristofolini, L., Witte, H., Schmid, O., Stokes, I., 2002. ISB recommendation on definitions of joint coordinate systems of various joints for the reporting of human joint motion – part I: ankle, hip, spine. Journal of Biomechanics 35, 543-548.

Wu, G., van der Helm, F.C.T., Veeger, H.E.J., Makhsous, M., Van Roy, P., Anglin, C., Nagels, J., Karduna, A.R., McQuade, K., Wang, X., Werner, F.W., Buchholz, B., 2005. ISB recommendation on definitions of joint coordinate systems of various joints for the reporting of human joint motion – Part II: shoulder, elbow, wrist, hand. Journal of Biomechanics 38, 981-992.

Zatsiorsky, V.M., Seluyanov, V.N., Chugunova, L.G., 1990. Methods of determining massinertial characteristics of the main segments of the human body. In Biomechanics VIII-B (Edited by Matsui, H. and Kobayashi, K.), Human Kinetic, Illinois, 1152-1159.